CERTIFICATE OF EXAMINATION

This is to certify that the dissertation titled **"Solvothermal Synthesis of Single Crystalline Palladium Nanocubes with Excellent Catalytic Efficiency"** submitted by Ms. Nayana C B (Reg No. MS14128) for the partial fulfilment of BS-MS degree programme of the Institute, has been examined by the thesis committee duly appointed by the Institute. The committee finds the work done by the candidate satisfactory and recommends that the report be accepted.

Dr. Sugumar Venkataramani Dr. Sanjay Singh Dr. Ujjal K Gautam

(Supervisor)

DECLARATION

The work presented in this dissertation has been carried out by me under the guidance of **Dr. Ujjal K Gautam** at the Department of Chemical Sciences, Indian Institute of Science Education and Research Mohali.

This work has not been submitted in part or in full for a degree, a diploma, or a fellowship to any other university or institute. Whenever contributions of others are involved, every effort is made to indicate this clearly, with due acknowledgement of collaborative research and discussions. This thesis is a bonafide record of original work done by me and all sources listed within have been detailed in the bibliography.

Nayana C B

MS14128

Date:

Place:

In my capacity as the supervisor of the candidate's project work, I certify that the above statements by the candidate are true to the best of my knowledge.

Dr. Ujjal K Gautam

(Supervisor)

Date:

Place:

ACKNOWLEDGEMENT

With great pleasure and reverence, I express my deep sense of gratitude, respect and obligation to my project supervisor Dr. Ujjal K Gautam (Department of Chemical Sciences, IISERM) for his excellent guidance, constant support, fruitful discussions and invaluable suggestions. His enthusiasm in research and timely criticisms have always been guiding light for me throughout my research project and plays a vital role in molding myself as an innovative researcher towards the future.

I express my sincere thanks to Prof. Arvind (Director, IISERM), Prof. Debi Prasad Sarkar (Former Director, IISERM) and Prof. S. Arulananda Babu (Head, Dept. of Chemical Sciences, IISERM) for providing excellent research facilities in IISER, Mohali. I would like to thank my committee members Dr. Sanjay Singh and Dr. Sugumar Venkataramani for their help and encouragement.

I am indebted to Lipipuspa for her adroit guidance, encouragement and wholehearted support. My heartfelt thanks are due to Sanjit, Kaustav, Nihal, Reeya, Maqsuma, Raj for their unconditional support, cooperation, guidance, suggestions and friendly atmosphere in the lab.

Finally, I have no words to express my gratitude and I'm forever indebted to my parents, teachers and friends for their encouragement and support throughout my academic career. Above all I bow before The Almighty for His immense blessing throughout my life.

List of figures

List of tables

Abbreviations

λ	Wavelength
K	Rate constant
M	Molarity
NC	Nanocube
CNF	Carbon nanofiber
TOF	Turnover frequency
NP	Nitrophenol
AP	Aminophenol
Sec	Second
Min	Minute
Hr.	Hour
Nm	Nanometer
A^0	Armstrong
Approx.	Approximately
g	Grams
mg	Milligrams
ml	Milliliter
Pd	Palladium
SEM	Scanning Electron Microscope
TEM	Transmission Electron Microscope
NMR	Nuclear Magnetic Resonance
rpm	Revolutions per minute

Contents

Abstract

Size and shape selective synthesis of noble metal nanoparticles plays a pivotal role towards the improvement of kinetics of various organic and inorganic transformations. However, the yield of the monodisperse nanostructure synthesized using various procedure achieved so far is not up to mark[1]. The main aim of this work is to synthesize monodisperse Pd NCs in high yield. As synthesized Pd NCs were investigated for catalytic reduction of 4-Nitrophenol and Suzuki-Miyaura coupling reactions as model systems. High catalytic efficiency of Pd NCs due to the presence of {100} facets, which have low activation energy, which in turn favors dissociative chemisorption of substrates. The reason for choosing aforementioned model systems is due to the ease in handling them and due to their impact in solving some serious environmental as well as industrial concerns. With the help of solvothermal synthesis, we have generated high yield of monodisperse Pd NCs below 10 nm . 4-Nitrophenol reduction followed Pseudo first order reaction with a rate constant of 3.129 min^{-1}, which is far better than many catalysts that have been reported so far. We further verified the catalytic activity using other aromatic nitro compounds as well. Along with these, we have highlighted the remarkable recyclability of our catalyst using cycles of 4-Nitrophenol reduction reactions. From our series of reactions, we discovered that Pd NCs can catalyze Suzuki- Miyaura coupling reaction at room temperature in short time period providing high yield of cross coupled product without any side reactions. Our catalyst shows superior catalytic activity in terms of efficiency and recyclability, which shows green light for its diverse catalytic applications in near future.

1. Introduction

1.1. Palladium Nanocube synthesis

"Metal nanoparticles are submicron scale entities made of pure metals as we can see from figure1 (e.g., gold, platinum, silver, titanium, zinc, cerium, iron, and thallium) or their compounds (e.g., oxides, hydroxides, sulfides, phosphates, fluorides, and chlorides)**"**[2]

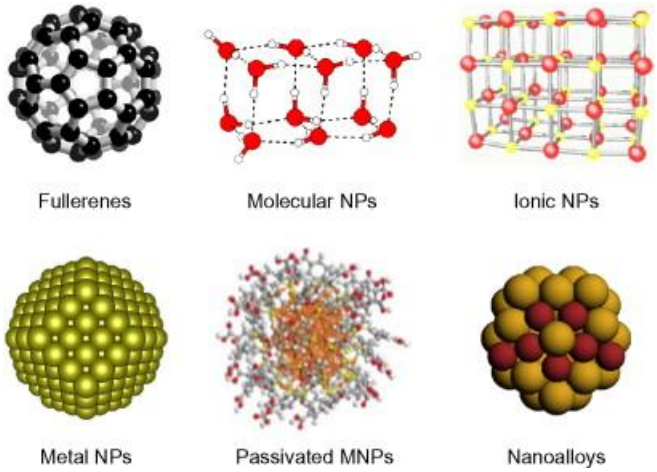

Fig 1. Metal nanoparticles and nanoalloys[3]

Metal nanoparticles are potential candidates for several applications. This is mainly due to their large surface-to-volume ratio and the quantum confinement effect[4,5] which happens when size of the particle is too less when compared to De Broglie wavelength of the electron. It will lead to a transition from continuous to discrete energy levels resulting in confinement of free electrons of nanoparticles. As a result, specific size-dependent catalytic, optical, electronic, and magnetic properties will be generated, opening up door for diverse applications in Physics, Chemistry, Biology and other Interdisciplinary fields. The applications of the nanoparticles, are also dictated by their shape, composition, crystallinity and surface functionality. For example, {100} facets have low activation energy, which in turn favors dissociative chemisorption of substrates.[6] So, by developing suitable shaped nanoparticle with more {100} facets (for instance, cube), will result in better catalytic activity[7]. By fine tuning different parameters, we can attain materials with desired properties. Therefore, the focus on precisely controlling shape and to understand their chemical behavior are crucial for better economic and performance efficiency of nanomaterials designed for diverse applications. Polymer, micelles, and coordinative ligands have been widely used as stabilizers in order to generate certain characteristic properties of nanoparticles.

Noble metals have been the point of interest of scientists from many centuries due to their remarkable resistance to corrosion and oxidation in moist air. Their several unique characteristics translates to their vital role in the development of chemical synthesis as we can see in figure 2.

Why noble metals are good catalysts?[8]

- Stability of noble metals makes them relatively inert toward reactants.
- Noble metals are resistant to oxidation by atmospheric oxygen while other reactive metal may not be so.
- Their ability to readily switch between two-electron oxidation-states plays an essential role in many catalytic reactions
- Their Pi bond acidity makes reactions used to generate molecular complexity proceed via pi bond activation
- Due to their notable stability, catalytically relevant precious-metal complexes are often capable of being isolated and reused.

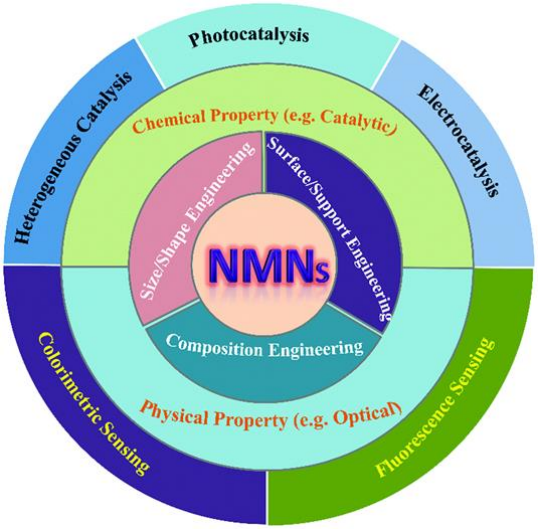

Fig 2. Schematic illustration of three strategies that can be used to tailor the physicochemical properties of noble metal nanoparticles, and the use of these physicochemical properties for several emerging applications [9]

Not many metals in periodic table can be called as 'noble'. They comprise Ruthenium (Ru), Rhodium (Rh), Palladium (Pd), Silver (Ag), Osmium (Os), Iridium (Ir), Platinum (Pt), and Gold

(Au). Among them d^8 metals are catalytically very important due to their unique characteristics. Due to their stable d^8 and d^{10} configurations, their 0 and +2 oxidation states have relatively less activation barrier when compared to other metals as we shown by figure 3. For the catalytic reactions having oxidative addition and reductive elimination, these oxidation states are really important. The lower activation barrier ensues in more rapid reactions, which in turn results in high rate constant for the catalyst.

Fig 3. d orbital energy levels of normal metal vs d^8 metals (Source: https://i.imgur.com/53jIl.png)

Goldilocks analogy is highly relevant in the case of Palladium and nearby metals. If metal is too reactive, it would adsorb substrates, get oxidized by itself and prefers to stay that way by holding the reactants back. But too much inertness also creates problem. They might not have any interest in adsorbing anything else. In that sense, d^8 metals are perfect choice due to their optimum reactivity which help them to hold onto reactants, allow them rearrange into products and permit them to leave once reaction is done. While both Palladium and Platinum have been center of attraction since long time, due to the high cost of Platinum, many scientists have been trying to focus more on applications of Palladium. Amount of metal can be effectively reduced without compromising potential applications by developing nanostructures.

The role of Pd nanoparticles in hydrogen storage due to its exceptional sensitivity toward hydrogen, as the primary catalyst for the reduction of pollutants emitted from automobiles, and in facilitating organic reactions such as Suzuki, Heck, and Stille couplings have already been discovered since long ago[10]. The main focus of this work is to generate Pd NCs and investigate

their potential catalytic applications.[11 12 13 14 7] Palladium nanocube can be described as a piece of single crystal of Palladium, which is bound by {100} facets. Similarly, nanocrystals enclosed by equivalent {111}, and {110} facets will form octahedron, and rhombic dodecahedron (RD), respectively. So much effort and resources have been spent so far to synthesis perfect shapes of nanomaterials, but it turns out to be really difficult and complex. Same method and reactants can give extremely different result because of minute changes in reaction condition.

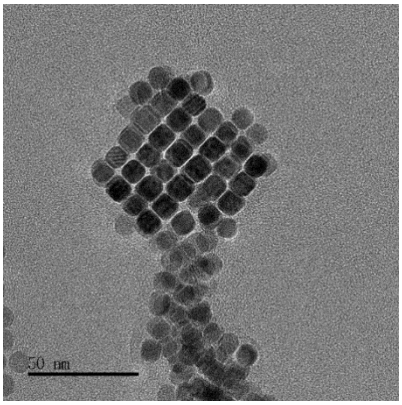

Fig 4. TEM image of Palladium nanocubes

For the synthesis of Pd NCs like what can see from figure 4, we need to use a suitable salt of Pd (for instance, Palladium Chloride, Palladium acetate, etc.). Suitable solvent and shape stabilizing agents like Poly (vinyl pyrrolidone) or Sodium dodecyl sulphate are also necessary. PVP can act both as a mild reducing agent and a good stabilizing agent to prevent the agglomeration of nanoparticles. Their reducing property is attributed by the presence of hydroxyl groups at the terminal positions of alkyl chains. In order to promote the formation of high-index facets, we can use long-chain capping agents. Long chains can be easily accommodated since high-index facets are less closely packed[13]. But we have to be careful about the amount and size of capping agents that we are using. Their excess size and concentration can mask active sites of catalyst, which will further shadow the catalytic activity in further applications. Effects of solvents on nanocube formation have also attracted attention of scientists, since it is observed that NCs will form in ethylene glycol only if Bromide ions are present, while in DMF, iodide ions are best for producing homogeneous NCs[15] . Fast nucleation by the addition of better reducing agents can also favor cube formation by bringing down time available to form twin defects.

Presence of halide ions is vital for controlling shape due to their preferential binding to {100} facets of various metals[16]. Figure 5 describes the adsorption behavior of Br- on the Pd {100} facets. As concentration of halide increases, the Palladium edges will be less exposed. This will bring down oxidative etching caused by Cl^- and O_2, the process by which the exposed Pd present in the edges of NCs will be oxidized to +2 oxidation state, resulting in the corrosion of edges. As the result of this process, cubes will be converted to irregular shapes and finally to spherical particles. Oxidative etching can be curtailed by adding oxygen scavengers like ascorbic acid. The chemisorption trend follows Chloride< Bromide< Iodide. Usage of different halides at varied amounts can generate diverse nanostructures. If we want to obtain NCs, Iodide ions will be better choice. As iodide ions can effectively mask the surface of NCs, they will be more resistant towards oxidative etching. In case of other halides, if we are unable to precisely modulate the concentration of halides, networked nanowires, nanobars nanoparticles, along with other nanostructures will be obtained.

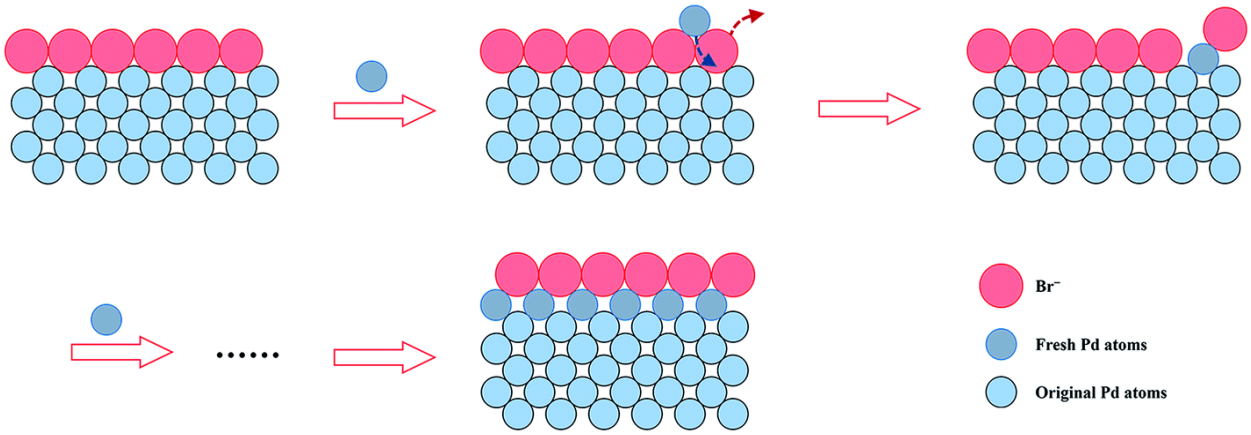

Fig 5. Possible growth pathway of the fresh Pd atoms onto the Br-capped Pd {100} facet.[17]

In solution phase, if Pd salt is reduced, nucleation of Pd atoms result in the formation of spherical particles (cuboctahedrons) enclosed by a mix of {100} and {111} facets. This process is thermodynamically favored. Generally, domination of thermodynamic factors results in the surface energy minimization, which in turn results in the formation of different shapes of nanocrystals[18] as we can see from figure 6. If bromide or iodide ions are present, they will chemisorb onto the surface of Pd seeds and alter the order of surface free energies for different facets, promoting the

formation of {100} facets. The palladium salts on {111} facets will be reduced, resulting in diminishing of those facets. This, along with the accelerated deposition of palladium atoms on the {100} facets will result in the growth of Palladium NCs. Anisotropic nanostructures like nanobars, structures with a square cross-section and enclosed by {100} facets, and nanorods, structures with an octagonal cross-section whose side surface is bounded by a mix of {100} and {110} facets, can be generated by kinetic control. Five-fold twinned structures can anisotropically grow into nanowires when their {100} facets are protected[13]. We can also generate high-index facets by kinetically controlling the atomic addition, making it uneven along the growth axis. High-index facets are highly valuable for catalysis due to the presence of lots of terraces and steps along with loosely packed surface atoms, making them highly reactive. Kinetic control of reaction condition involves varying the type and concentration of reducing agent, adding ionic species as well as optimizing the injection rate and the reaction temperature[19].

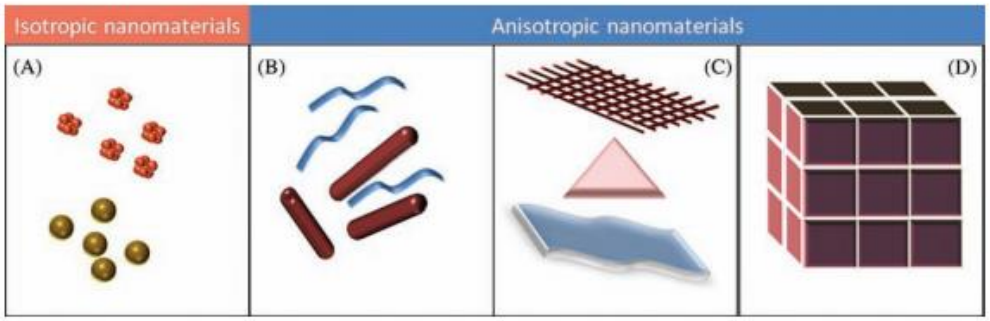

Fig 6. Various kinds of nanomaterials. (A) 0D spheres and clusters. (B) 1D nanofibers, wires, and rods. (C) 2D films, plates, and networks. (D) 3D nanomaterials.[20]

Different approaches are adopted for the efficient synthesis of Pd NCs. The most popular ones are Polyol method, seed mediated synthesis and hydrothermal synthesis.

1.1.1. Polyol method

In polyol method all the reagents along with ethylene glycol will be taken which acts as a solvent, reducing agent and stabilizer as schematically represented in figure 7. Ethylene glycol will reduce Palladium from +2 to 0 oxidation state. When we increase the temperature of reaction mixture, nucleation will take place due to increasing reduction

potential of ethylene glycol, which further result in the formation of metal nanoparticles. So many modifications of this method have been proposed so far. But it is still a great challenge to precisely control shape and size of nanostructures, especially those within sub-10 nm. Due to the usage of large amount of solvent, separating our product from it poses a great challenge, which will ultimately bring down the yield.

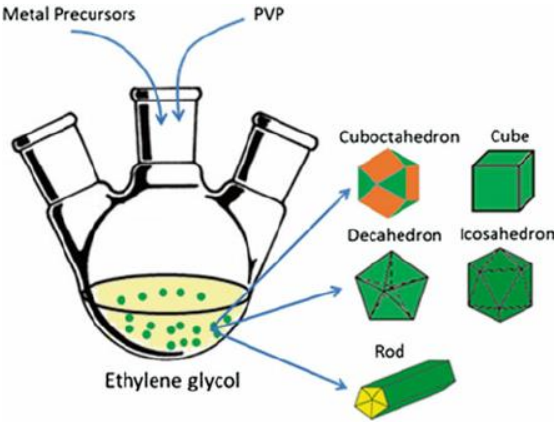

Fig 7. Schematic of the polyol method [21]

1.1.2. **Seed-Mediated Growth Method**[22]

In this method, a metal precursor is reduced small that will become seeds with a single-crystal, singly twinned, or multiply twinned structure, which further determines the final morphology as shown in the figure 9. The schematic representation of atom movement is illustrated through figure 8. If we want to obtain Pd NCs as end product, already synthesized Pd NCs are used as seeds in this approach. Size of the obtained NCs can be modulated by adjusting amount of seeds added. More seeds added, lesser will be the edge length of cubes formed due to the availability of more sites for further deposition. Size of seeds have to be big as the crystal structure fluctuates their size is very small, resulting in polycrystallinity. It has been observed that different amount of seed solution dictates the growth rate of Pd along <100> and <111> directions, for example, very less amount of seeds will result in the formation of cuboctahedrons. At medium concentrations of iodide ions, {110} facets will be favored at high temperature and {111} at relatively low temperature. At high temperature, more Palladium atoms will be generated without the surface catalysis of the added seeds. This spontaneous nucleation will ultimately result in nanorod

formation. Usually, KI can suppress spontaneous nucleation to some extent by facilitating the catalytic deposition of palladium atoms to the seeds that are already formed. As mentioned in polyol synthesis, difficulty in separation of nanoparticles from reaction mixture at the end of the reaction is challenging here as well due to presence of excess solvent.

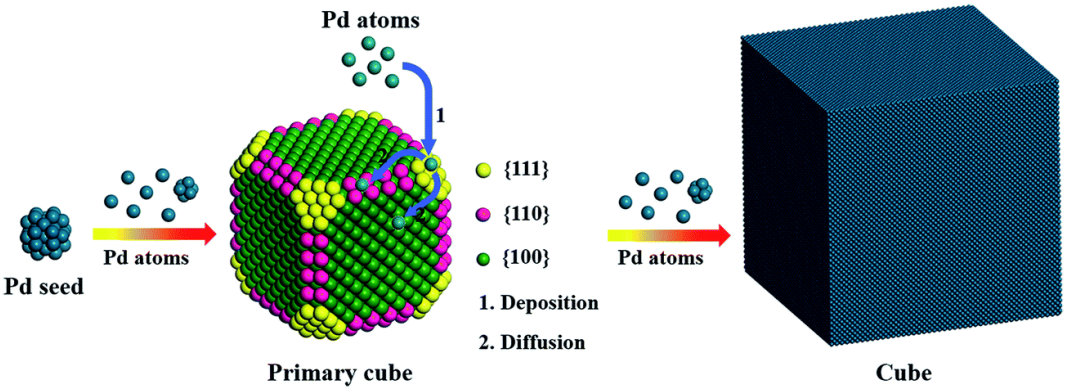

Fig 8. Schematic illustration of the atom movements during the growth process[17]

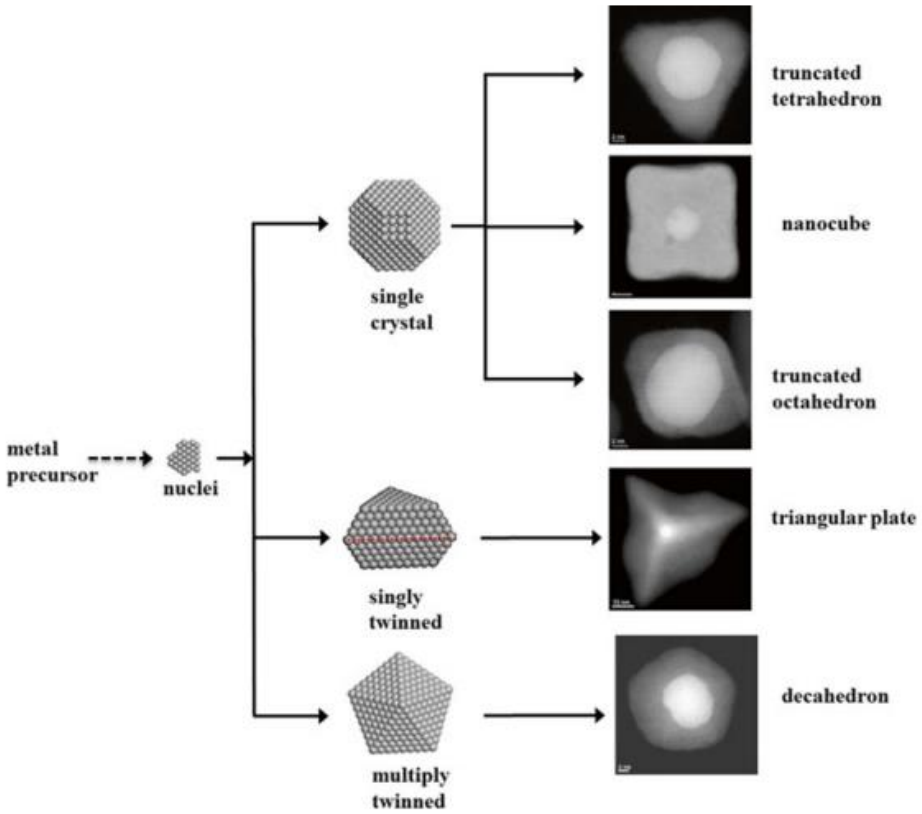

Fig 9. Reaction pathways that lead to face-centered cubic (FCC) metal nanocrystals having different shapes.[21]

1.2. Methods to investigate catalytic activity

Once catalyst is synthesized, our next aim is to investigate their catalytic efficiency. For this purpose, we have chosen 4- Nitrophenol reduction to 4- Aminophenol, as well as, Suzuki-Miyaura coupling reaction. The reasons for choosing these model systems have been discussed in details in results and discussions part.

1.2.1. 4-Nitrophenol reduction

4-Nitrophenol, a light-yellow solid with very little odor, is used mainly to manufacture drugs, fungicides, and dyes, and to darken leather. It can degrade in water and surface soil, but the breakdown takes longer at lower soil depths and in groundwater. The aggregation of amount of 4-Nitrophenol is alarming. Its main input is because hydrolysis of various pesticides and industrial wastes. It is listed as one of the "Priority Pollutants" according to United State Environmental Protection Agency (UESPA), because of its contamination of ground water resources. Agency for toxic substances and disease registry warns that 4-Nitrophenol can enter our body pass into the blood stream if we breathe contaminated air or drink water containing it. Chemicals like the nitrophenols cause a blood disorder in humans, along with methemoglobin formation, liver and kidney damage, anemia, skin and eye irritation, and systemic poisoning.[24] Therefore, presence of 4-Nitrophenol in our environment is of a significant concern and hence industrial waste water containing it should be treated before discharging, for both environmental protection as well as for sustainable development.

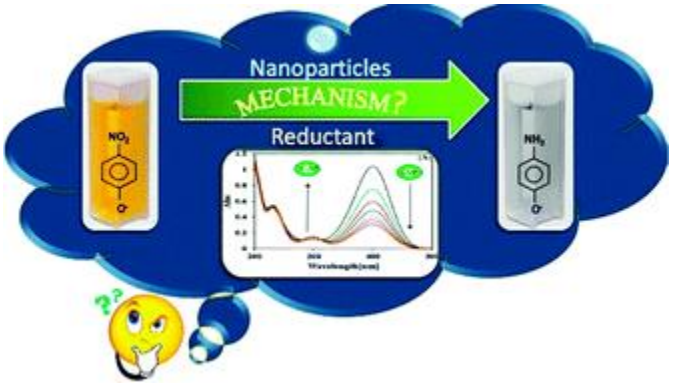

Fig 10. 4-Nitrophenol reduction [25]

Efforts to develop a highly efficient catalyst to reduce 4-Nitrophenol to 4-Aminophenol (Figure 10) have been an active research area since a very long time. While 4- Nitrophenol is a toxic pollutant, 4- Aminophenol is a compound that is useful in different fields of our daily life. Its wide range of applications involves its usage as photographic developer, hair-drying agent, anti-corrosion lubricant, corrosion inhibitor, weak acid dyes such as yellow 5G and it acts as a precursor for drugs like paracetamol and clofibrate.[26 27]

Catalytic hydrogenation is an efficient method for the generation of aromatic amines from aromatic nitro compounds because of several reasons like high and fast conversion rate, absence of side products and acid effluents are not generated as the part of the reaction. This method is widely used as a model reaction to study the catalytic activity of different metal nanomaterials and complexes, due to the easiness in monitoring the progress of the reaction and studying kinetics. This is like killing three birds with a single stone- hazardous aromatic nitro compounds can be depleted effectively, useful amino compounds can be generated efficiently, and finally catalytic activity of new Pd NCs can be monitored effortlessly.

The progress of the reaction is easily noticeable with the help of UV-Vis spectroscopy. Aqueous 4-Nitrophenol solution has yellow color and typically shows an absorption peak at 317 nm. When we add sodium borohydride to it, the solution turns even brighter yellow color and the peak get shifted to 340 nm, due to the formation of 4-nitrophenolate ion under alkaline pH. As we add catalyst, the reaction proceeds and we can see diminishing of color of the solution as well as peak at 340 nm vanishes, giving rise to another peak at 298 nm corresponding to the product.

This method of 4-Nitrophenol reduction is an irreversible six-electron transfer process in the presence of a reducing agent, sodium borohydride ($NaBH_4$). In this method, as shown in fig 11, 4-Nitrophenol is first reduced into nitroso intermediate, then to hydroxyl amine, the first stable intermediate, which further reduces to the p-Benzoquinone imine and finally to amino product. This reaction cannot take place without catalyst due to high activation barrier generated due to strong electrostatic repulsion between the reactant and the reductant. Metal catalysts like Pd, Ni, Re, Pt, TiO_2 in the presence of reducing agents like

$NaBH_4$ or NH_2NH_2 can catalyze the reaction. Here, both 4-nitrophenolate ion and borohydride ion get adsorbed onto the surface for the catalyst so that electron transfer can occur, thus crossing kinetic barrier.

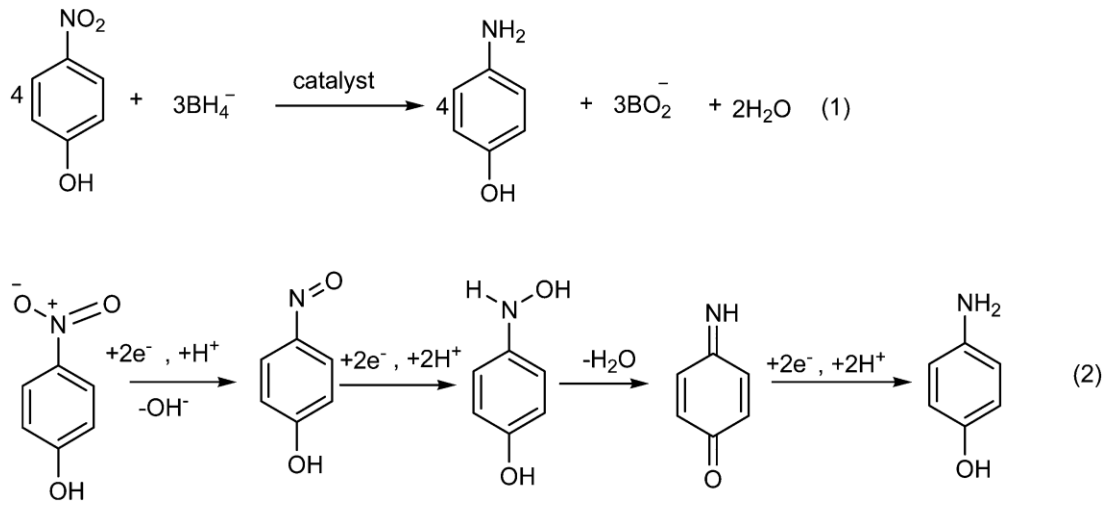

Fig 11. Mechanism of aromatic nitrophenol reduction. [28]

We need to study kinetics of the reaction to obtain rate constant of the reaction.[29] The kinetic equation of this reaction can be written as,

$$-\frac{\partial C_t}{\partial t} = k'[NaBH_4]^m(C_t)^n$$

where,

C_t = Concentration of 4-Nitrophenol at time t

k'= rate constant

m = reaction order of [$NaBH_4$]

n= reaction order of C_t

If we consider this this to be a second order reaction, finding rate constant will be too much complicated. When excess $NaBH_4$ is present along with sufficient amount of catalyst, the reaction is a pseudo-first-order reaction. In this case the rate of the reaction solely depends on the amount of 4-Nitrophenol present. Thus, above reaction can be simplified as,

$$-\frac{\partial C_t}{\partial t} = k(C_t)^n$$

Taking logarithm on both sides will yield,

$$\ln\left(\frac{C_t}{C_o}\right) = -kt$$

Here,

C_t = Concentration of 4-Nitrophenol at time t

C_0 = Initial concentration of 4-Nitrophenol

k = rate constant

According to Beer Lambert law, absorbance of a solution can be expressed as,

$$A = \varepsilon lC$$

Where,

A = Absorbance

Ɛ = Wave-length dependent absorptivity coefficient

l = Path length

C= Analyte concentration

At a particular λ_{max}, Ɛ and l will be constant. i.e., Absorption and concentration will be directly proportional. Therefore, our equation can be rewritten as,

$$\ln\left(\frac{A_t}{A_o}\right) = -kt$$

Here,

A_t = Absorbance at time t

A_0 = Initial Absorbance

k = rate constant

The graph between ln (A_t/A_0) vs t can be plotted and the slope gives the value of rate constant.

1.2.2. Suzuki- Miyaura Coupling

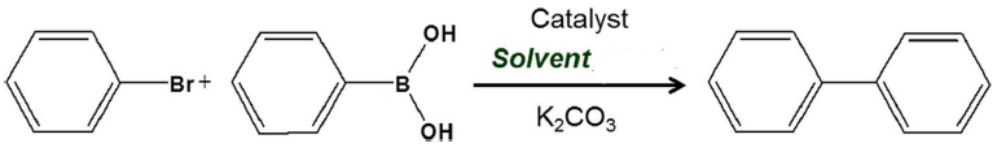

Fig 12. Scheme of Suzuki coupling reaction

Suzuki reaction as represented by figure 12, which was first reported in 1979 by Akira Suzuki, is a well-known as well studied reaction due to its importance in synthesis of intermediate complexes in pharmaceuticals, advanced materials, natural products and other industries. In this reaction, a single bond is formed between two carbon atoms by coupling an organoboron species with a halide using a palladium catalyst and a base. Even though this reaction was discovered decades ago and several modifications have been introduced since then, still there are many challenges that are faced while performing the reaction. When we are perusing through literature, we can see that most of the catalytic studies have been carried out in homogeneous systems. Solvent soluble palladium complexes are used for this method. Even though this method has many advantages such as requirement for lower temperature for the reaction than heterogeneous systems, they face several serious like difficulty in separating catalyst from reaction mixture once reaction is over, since all of them are in same phase. Since Palladium is not so cheap metal, recyclability is a necessary criterion if we want to use the catalyst industrially. In case of heterogeneous catalysis, catalyst and reactants are in different phase, so that we can filter out or centrifuge catalyst and reuse it again without losing significant amount of activity. But leaching out of metal ions into reaction media is a problem faced by this method. Suitable solid support can be used to counteract this. Currently, many scientists have been focused on generating heterogeneous catalysts which can perform this coupling reaction at high yield, low reaction temperature and time and high recyclability.

The general mechanism of this reaction using a Pd catalyst is shown in the scheme (Figure 13). Palladium in 0 oxidation state acts as active site in this process (**1**). The different steps

involved in this catalytic cycle involve oxidative addition, transmetalation and reductive elimination[30 31]. In the first step, organopalladium species will be formed by the insertion of Pd (0) between carbon halogen bond of aryl halide R_2-X as shown in the scheme. This addition leads to the oxidation of Palladium species from 0 to +2, hence the process is called oxidative addition (**2**) resulting in the formation of (**3**). This is followed by activation of Palladium center along with elimination of halide ion with the help of a suitable base like K_2CO_3 or NaO^tBu (**4**). Along with this, base will also coordinate with boron in phenyl boronic acid (**5,6**) and makes the R_1 group more nucleophilic, which in turn facilitates the transmetalation step[32 33], in which R_1 group is eventually transferred to palladium center (**8**) leaving out the boron complex (**7**). In the final step, C-C bond will be formed by the reductive elimination of Palladium species (**9**), which will be ready for next catalytic cycle (**1**).

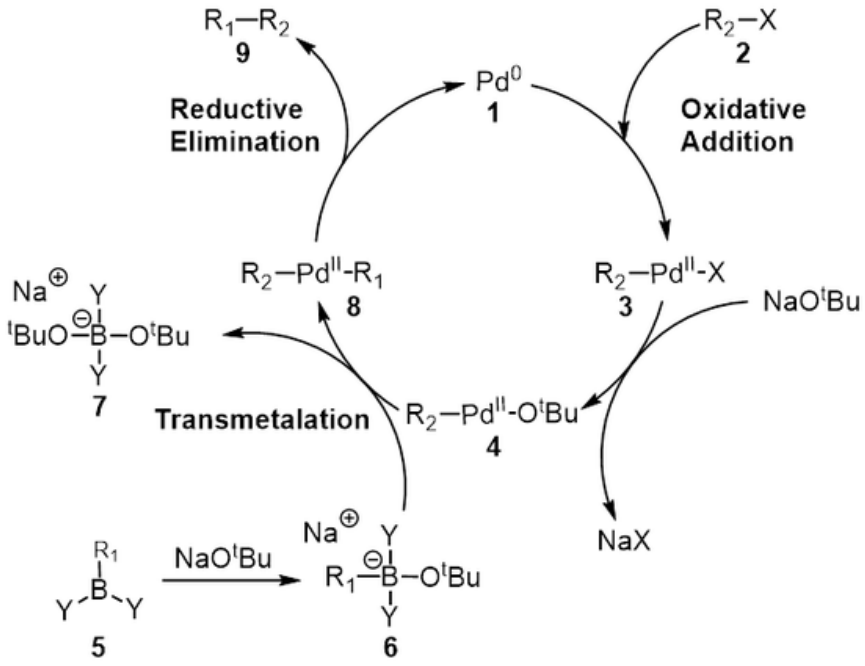

Fig 13. Mechanism of Suzuki coupling (Source: Wikipedia)

2. Experimental Section

2.1. Chemicals: Palladium (II) Chloride ($PdCl_2$, 99.9%, metals basis, Pd 59.0% min crystalline), Poly (vinyl pyrrolidone) (PVP, Mol wt. 40,000, Sigma -Aldrich), Sodium iodide (NaI, Himedia, Hi-AR/ACS), Concentrated Hydrochloric acid (Conc. HCl, Himedia, 35% pure, Hi-AR), 4-Nitrophenol ($C_6H_5NO_3$, Sigma Aldrich, ≥99%), 2-Nitrophenol ($C_6H_5NO_3$, Honeywell, ≥99%), 2,4-Dinitrophenol ($C_6H_4N_2O_5$, Sigma Aldrich, ≥99%), 3-Nitrophenol ($C_6H_5NO_3$, Sigma Aldrich, ≥99%) , 4-Nitroaniline ($C_6H_6N_2O_2$, Sigma Aldrich, ≥98%), 2-Hydroxy-5-nitrobenzaldehyde ($C_7H_5NO_4$, Sigma Aldrich, 98%), Picric acid ($C_6H_3N_3O_7$, Sigma Aldrich, ≥98%), Sodium borohydride ($NaBH_4$, Fluka Analytical, ≥99%) , Absolute ethanol (C_2H_5OH, Ensure ACS, ISO, Reag. Ph Eur), Acetone (C_3H_6O, Rankem LR), Isopropanol (C_3H_8O, Merck, 99%), Ethanol (C_2H_5OH, AR 99.9%, Changshu Hongsheng Fine Chemical Co., Ltd.), Methanol (C_2H_4O, Rankem LR), Hexane (C_6H_{14}, Rankem LR), Ethyl acetate ($C_4H_8O_2$, Rankem LR), Chloroform ($CHCl_3$, Himedia, AR), Chloroform D + 0.03% Tetramethyl silane ($CDCl_3$+0.03% $C_4H_{12}Si$, Euriso-top) Dichloromethane (CH_2Cl_2, Rankem, LR), Silica gel (SiO_2, 100-200 mesh, Merck), Aluminium oxide active, neutral (Al_2O_3, 70-230 mesh, Himedia), Potassium carbonate anhydrous (K_2CO_3 anhy. 99%, Extra pure, Loba Chemie), Phenyl boronic acid ($C_6H_7BO_2$, Alfa Aesar, 98+%), Iodobenzene (C_6H_5I, Aldrich Chemistry, 98%), 1-Iodo-4-nitrobenzene ($IC_6H_4NO_2$, Alfa Aesar, 98+%), 4-Iodoanisole ($IC_6H_4OCH_3$, Alfa Aesar, 98+%). The distilled water used was taken from Milli-Q purification system with resistance 18.2 MΩ cm^{-1}.

2.2. Synthesis of Palladium nanocubes

Pd NCs were prepared using hydrothermal synthesis. Palladium (II) Chloride (22.5 mg) is taken in an eppendorf and 3 drops of conc. Hydrochloric acid was added to it and sonicated for 30 minutes. This results in the formation of H_2PdCl_2, to which 4 ml H_2O was added. Meanwhile, 9 ml of water was added to 1g of 40K Poly (vinyl pyrrolidone) taken in a 50 ml beaker and vigorously stirred at room temperature until it was completely dissolved in the solution. Here PVP is in excess when compared to the amount of $PdCl_2$. Both solutions were mixed together thoroughly. After 5

min of stirring, freshly prepared 2ml of Sodium iodide in H_2O solution, whose concentration was optimized, was added dropwise. Followed by additional stirring of 20 minutes, the resulting homogeneous dark brown solution was transferred to a 25 ml Teflon-lined stainless-steel autoclave and the sealed vessel was kept at 200^oC. The reaction was allowed to proceed for different periods of time for further optimization. Once the reaction was completed, the autoclave was cooled to room temperature and the dark brown colored solution was centrifuged at a rate of 13,500 rpm for 30 min to collect the black colored Pd NCs, followed by washing with water several times and then with ethanol once to remove unreacted reagents, if remaining and excess PVP. The precipitates were redispersed in ethanol and were characterized by transmission electron microscopy (TEM).

2.3. Nitrophenol reduction

2.7 ml of 0.1 mM 4- Nitrophenol along with 0.3 ml of 0.6 M of $NaBH_4$ were taken in a cuvette and 1 µl of 1mg/ml aqueous dispersion of catalyst was added to it, stirred, and UV spectra and kinetics were recorded. Same procedure was followed for the reduction of other aromatic nitro compounds. In order to check recyclability of our catalyst and effect of temperature on it, we have performed the same set of above reaction, along with addition of 27µl of 4-Nitrophenol after each catalytic cycle.

2.4.Suzuki Coupling

In a general method, a 10 ml one-neck round-bottom flask was charged with aryl halide (1 mmol), phenylboronic acid (1.2 mmol), potassium carbonate (2 mmol), Pd NCs dispersed in EtOH (250µl corresponding to 0.3 mg), and a mixture of ethanol and water (1:1, 4 ml). The solution was then stirred for the desired time at room temperature. In order to monitor the progress of reaction, an aliquot was taken in a small Eppendorf at arbitrary time intervals, water and ethyl acetate was added to it, and organic layer was analyzed using TLC (Thin Layer Chromatography) technique. Vanishing of reactant spots in TLC plate indicates the complete conversion of reactants to product. Presence of single product spot verifies the absence of any plausible side reaction. Once reaction was completed, the ethanol present in the reaction mixture was evaporated using rotavapor. The reaction mixture was purified with the help of separating funnel, using ethyl acetate and water as solvents. The catalyst can be separated along with the aqueous layer. The organic layer was

evaporated under reduced pressure to obtain our required biaryl compounds and further isolation and purification of product was done with the help of Column chromatography.

2.5.Materials Characterization

Scanning electron microscopy (SEM) images were obtained using a field emission microscope (FESEM, JEOL, JSM- 7600F). The FESEM was operated with an accelerating voltage of 20-30 kV and a chamber pressure of 10^{-5} Torr. All SEM samples were prepared by drop casting ethanolic solutions of the sample on silicon wafers and allowing the solvent to evaporate slowly at room temperature in a vacuum desiccator. Transmission electron microscopy (TEM) and electron microdiffraction patterns were obtained using a FEI TITAN3TM electron microscope using an accelerating voltage of 80-300kV. In order to prepare samples for TEM, drops of diluted solutions were placed on Formvar- coated, copper TEM grids. The drop casted grids were kept in vacuum desiccator to completely evaporate the solvent. UV-Vis absorption spectra were recorded using a LABINDIA UV-Vis spectrophotometer at room temperature. NMR spectra were taken using 400 MHz Spectrometer operating under 9.397 Tesla field strength manufactured by Bruker Biospin Switzerland.

3. Results and discussion

This work mainly involves three main parts. Our main aim is to synthesize monocrystalline Pd NCs at high yield and to further investigate their potential catalytic application as well as efficiency by using 4-Nitrophenol reduction and Suzuki-Miyaura coupling reactions as model systems. Recyclability of our catalyst was verified using the former model system.

3.1. Synthesis of Palladium nanocubes

Several factors play crucial role in regulating size and shape of nanostructures. Reproducing same results under same reaction conditions may not be easy as it seems. While one factor favors increase in size, another will do reverse. All parameters have to be optimized and act in perfect symphony to achieve desired nanostructure. As we discussed in the introduction part, commonly used methods for the NC generation is highly flawed due to sparse yield. So, we decided to explore about another synthetic route, i.e. Solvothermal synthesis

3.1.1. **Solvothermal synthesis**[23]

There are a few reports on this method. But those reports mention the necessity of using more expensive solvents[15] or additional shape regulating agents like SDS(Sodium dodecyl sulfate) along with PVP and halide salts[34]. But we discovered that, by just optimizing the amount of NaI, we can synthesize remarkable yield of Pd NCs using just water as solvent In this method, metal precursor along with PVP, halide salt and suitable solvent are mixed properly and transferred to a Teflon-lined stainless-steel autoclave(Figure 14) and the sealed vessel will be kept at high temperature for an optimized amount of time. Main advantages of this method are that, we can precisely control the size, shape and crystallinity of the nanocrystals that are forming by optimizing different parameters like time of reaction, temperature, fill volume, pH, type and amount of precursor, stabilizer, reducing agent, solvent and so on. Through this method, syntheses of some low-temperature phases and metastable compounds can be possible, which may not be possible through some other methods. Some transition metal complexes with some oxidation states that are difficult to attain can also be achieved through this way of synthesis.

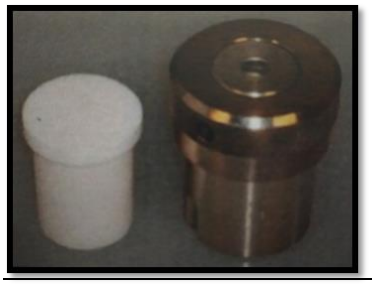

Fig 14. Autoclave for solvothermal synthesis

Understanding different steps involved in the reaction process comes first. $PdCl_2$ is the starting material used, but it is not soluble in water which is used as the solvent for nanocube synthesis. So, we need to make it soluble in water first. When Palladium salt is sonicated in conc. HCl, it will form H_2PdCl_4, that is soluble in water. Here balanced amount of chloride ions matters a lot. Addition of very little may not be sufficient, while excess addition facilitates oxidative etching once cube is formed, thus resulting in polydispersity which is not desirable.

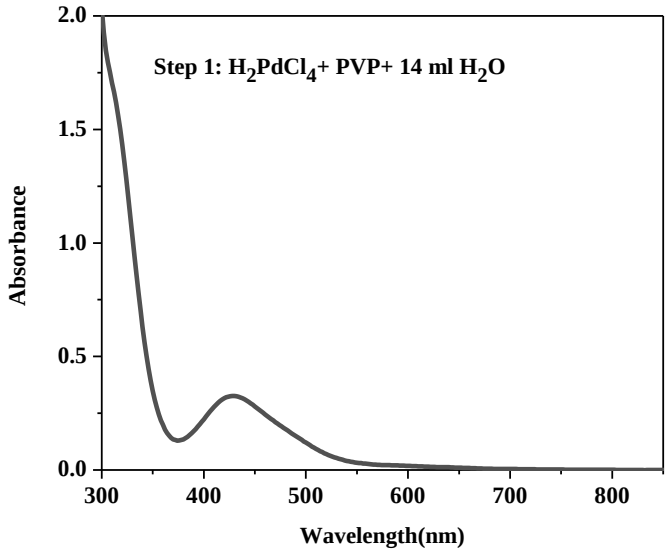

Fig 15. UV adsorption spectrum of aqueous solution of H_2PdCl_4 along with PVP

The peak at 425 nm corresponds to that of aqueous solution of H_2PdCl_4 along with PVP[35] as shown in Figure 15. Once we add Sodium iodide solution, chloride ions initially present will be replaced by iodide ions which are more heavier resulting in the formation of H_2PdI_4, which in turn lowers the potential of the palladium species. This will result in slow reduction and thus

prevents defects due to spontaneous reduction. Under suitable reaction conditions for optimized amount of time, Palladium from +2 oxidation state will be reduced to 0 state and will be rearranged to form nanostructures.

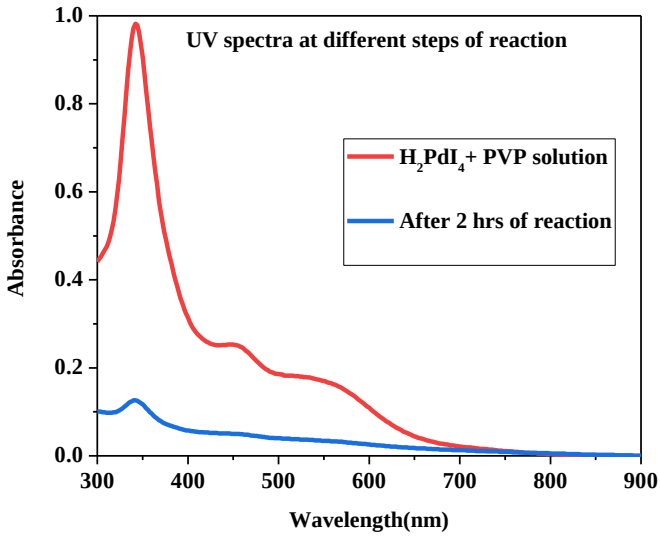

Fig 16. UV adsorption spectrum of reaction mixture just after the addition of NaI and after 2 hours of reaction

Presence of peak around 350 nm along with two peaks observed in between 400 and 600 nm indicates the formation of H_2PdI_4 [36]as well as the gradual disappearance of peak at 425 nm indicates the consumption of H_2PdCl_4 species as indicated by figure 16. After the reaction for optimized amount of time, the vanishing of peaks of H_2PdI_4 are apparent. This confirms that H_2PdI_4 has been consumed in the reaction to form palladium nanostructures.

The overall process can be consolidated into the following reaction scheme (Figure 17)

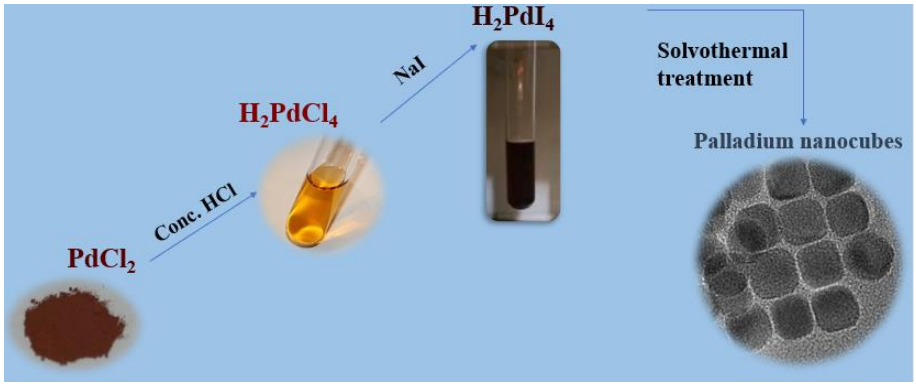

Fig 17. Schematic representation of the formation of Palladium nanocubes

Here the resultant shape of nanostructure depends a lot of concentration of iodide ions, which will preferentially get adsorbs in the {100} facets and shields from further oxidative etching. The single crystal with {100} facets is cubical in shape. Solvent cannot be neglected as well. Viscosity of solvent affects reaction dynamics in general, while solvents like ethylene glycol having hydroxyl functional groups act as reducing agent as well. Poly (vinyl pyrrolidone) also acts as a mild reducing agent as well as capping agent, which prevents further agglomeration.

3.1.2. Role of halide precursors

Halide ions can act as capping agents and thus facilitates cube formation. But, high electronegativity of Chloride ions results in corrosion of edges of NCs. So, Chloride salt was omitted from choice. In order to check how other two halides are giving results, we have used NaBr and NaI. Usually for Polyol method of synthesis, NaBr can give good yield of cubes. Our choice of method was Solvothermal since, less amount of solvent is required in this method when compared to other methods. This favors minimal loss of product during centrifugation, which is an important advantage since metal precursor is not so cheap. But there are reports that NaBr salt alone cannot give homogeneous shape and size distribution, giving rise to the necessity of additional capping agents like Sodium dodecyl sulfate[34]. To check whether this claim is true, we used NaBr+ SDS also. Results obtained were same as that we were expecting. In all of these three experiments, we used 22.5 mg $PdCl_2$, 3 drops of conc. HCl, 1 gm PVP, 15 ml H_2O and 25 ml autoclave containing reaction mixture was kept at 200^oC for 2 hrs.

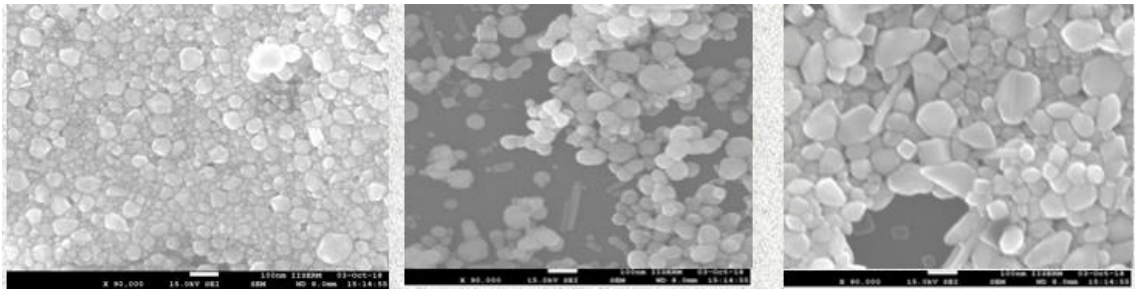

Fig 18. SEM images of Palladium nanostructures generated in the presence of 2.5 mmol of (a) NaBr (b) NaBr + SDS (c) NaI

As we can see from the figure 18, Polydispersity and heterogeneous size distribution is generated which can be minized only through further optimization. Among these three, only NaI is generating some cubes. Theoretically, chemisorption of halides increase in the order Chloride< Bromide< Iodide. This makes Iodide ions better candidate since, it can efficiently mask exposed facets of Palladium. Minute changes in NaBr concentration alters shape of nanostructure because of its higher corrosive nature than iodide ions due to electronegativity. So we decided to further optimize the amount of iodide salt concentration.

3.1.2 Optimization of amount of NaI added

Once the salt is finalized to be NaI, the next step is to investigate its balanced concentration requires for nanocube formation. Starting from 0.83mmol, we have tried different amount of salt such as 2.5 mmol, 7.5 mmol,12.5 mmol and 17.5 mmol to see how this change is going to affect the shape. In all of these experiments up to 7.5 mmol, we used 22.5 mg $PdCl_2$, 3 drops of conc. HCl, 1 gm PVP, 15 ml H_2O and 25 ml autoclave containing reaction mixture was kept at 200^oC for 2 hrs. For higher concentrations of NaI, after just 2 hrs., particles were not settling down by centrifuging it at 13,500 rpm form 1 hr. So, we gave extra 10 hrs. at same reaction conditions to obtain product.

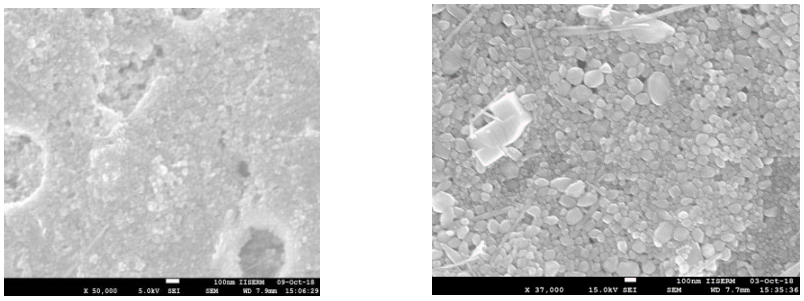

Fig 19. SEM images of Palladium nanostructures generated in the presence of (a) 0.83mmol NaI (b) 2.5 mmol NaI

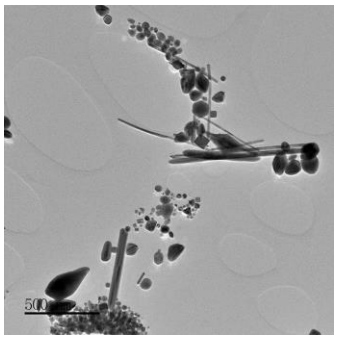

Fig 20. TEM images of Palladium nanostructures generated in the presence of 2.5 mmol NaI

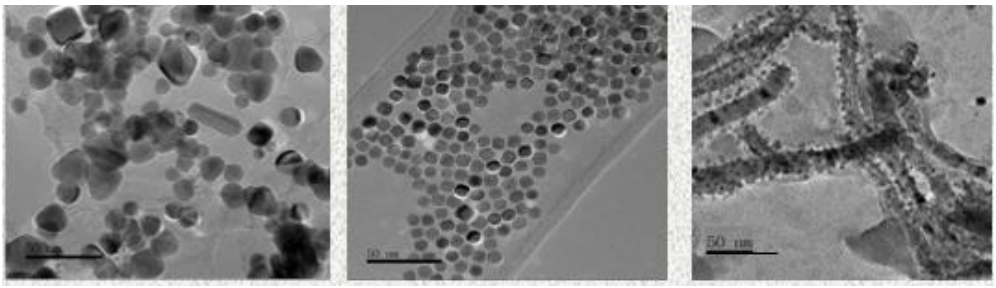

Fig 21. TEM images of Palladium nanostructures generated in the presence of (a) 7.5 mmol NaI (b) 12.5 mmol NaI (c) 17.5 mmol NaI

At lower concentrations of NaI, the iodide ions are not sufficiently enough to shield NCs completely from oxidative etching. This will result in polydispersity as shown in the figure 19 and 20. The amount of NaI can tune the percentage of {100} facets. At very high concentrations of NaI, nanowires will be formed due to anisotropic growth when their {100} facets of cubes are protected, by an autocatalytic process. From the string of experiments, we noticed that the optimum amount of NaI required at the considered set of parameters turns out to be 12.5 mmol (Figure 21).

3.1.3. Optimization of time required for the synthesis

When we provided 2 hrs for the solvothermal method of synthesis of Pd NCs, particles were not properly settling down. So we tried to provide additional 6 hrs to the same reaction mixture. We tried to give straight 8 hrs instead of providing 2 hrs first, waiting for the autoclave to cool down, then providing an additional 10 hrs. The result was

surprising. As the TEM images in figure 22 shows, the nanostructures formed in the latter process was more closer to spheres than cubes. In both of these experiments, we used 22.5 mg $PdCl_2$, 3 drops of conc. HCl, 1 gm PVP, 12.5 mmol NaI, 15 ml H_2O and 25 ml autoclave containing reaction mixture was kept at 200^oC .

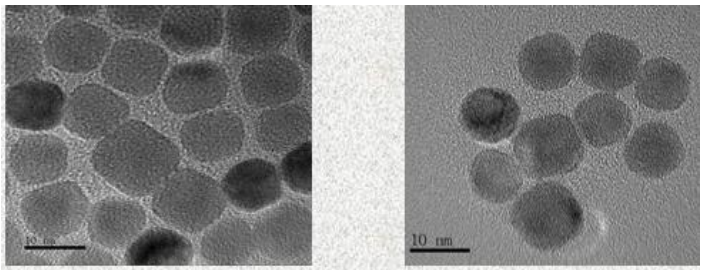

Fig 22. TEM images of Palladium nanostructures generated when time provided for the reaction is (a) 2+ 6 hours (b) 8 continuous hours.

The plausible reason might be seed formation in the first reaction. After 2hrs of reaction, the reduced palladium species will form templates for NCs onto which further addition takes place when it is kept further under solvothermal setup. When reaction is stopped at 2 hours, iodide ions will cover the facets of cubes and further oxidative etching is halted. As soon as we will proceed with the reaction, additional H_2PdI_4 present in the reaction mixture will be reduced, while it takes time for deposited Palladium species to get oxidized since facets exposed will be less. So further addition will be faster than deposition. But in the second case, both deposition and corrosion will take place simultaneously resulting in the formation of spherical particles rather than cubes as illustrated by figure 23. If we reduce overall reaction time, yield will be less since most of H_2PdI_4 will be remaining in the solution unreduced.

Fig 23. Illustration showing how nanocube will get converted to spherical shape as reaction goes on.

3.1.4. Overview on optimum conditions for obtaining nanocubes

3 drops of conc. HCl should be added to 22.5 mg of $PdCl_2$ to prepare H_2PdCl_4 solution. Amount of PVP and NaI were optimized to be 1g and 12.5 mmol respectively. The total volume of H_2O required to make reaction mixture was estimated to be 15 ml, when we are using 25 ml autoclave. The sealed vessel has to be kept at 200^oC for 2+6 hours to obtain NCs. Once reaction is over, Pd NCs can be separated from the reaction mixture by centrifuging at 13,500 rpm for 30-60 min.

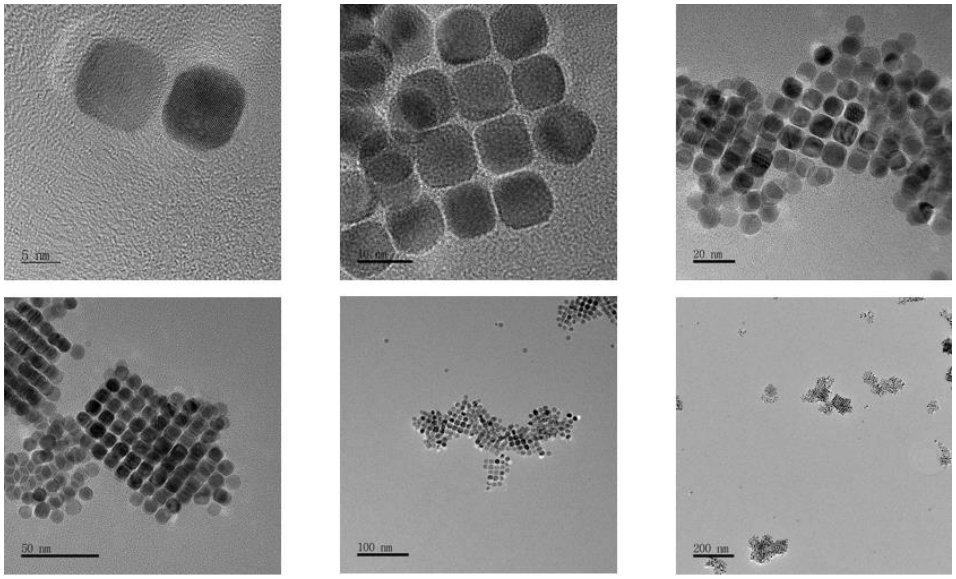

Fig 24. TEM images of Palladium nanostructures, generated in the optimized reaction conditions, at different magnifications.

3.2. 4-Nitrophenol reduction using as synthesized catalyst

Once NCs were obtained, our next aim was to investigate their potential catalytic activity. As we have already discussed in the introduction, one of the useful ways is to check its 4-Nitrophenol reduction efficiency as indicated by figure 25. In the presence of $NaBH_4$ and catalyst, 4- Nitrophenol will be reduced to 4- aminophenol, without the formation of any side products. The only instrument needed to measure the catalytic efficiency is UV-Spectrophotometer. The absorption peak of 4-Nitrophenol along with Sodium borohydride solution at 400 nm along with the yellow color of solution vanishes as the reactant gets

converted to product. The isosbestic point obtained from the spectra further refutes the presence of any possible side product.

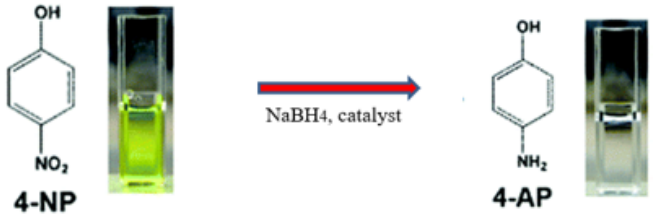

Fig 25. Reduction of 4-Nitrophenol to 4- Aminophenol

Even though the main reason for choosing 4-Nitrophenol reduction as a model system is because of its idealness in indicating of how good our catalyst is, the reaction itself has lot of relevance as we have already discussed in the introduction.

3.2.1. Reaction conditions and method of calculation of rate constant

2.7 ml of 0.1 mM 4-Nitrophenol was used for the reaction, which means that 0.27 µmol of reactant is present. Since this reaction is a second order reaction and we want to conduct it as a pseudo first order reaction, one of the reactants have to be in excess. So, 0.18 mmol of Sodium borohydride was used, i.e., 0.3 ml of 0.6 M $NaBH_4$ solution. In order to verify whether Pd NCs show superior catalytic activity over other palladium nanostructures, we reduced 4-Nitrophenol using each of the catalyst that we generated throughout the journey of optimization of nanocube synthesis. All the reactions were performed at room temperature using water as solvent. In order to monitor the vanishing peak of reaction mixture at 400 nm, we added 1µl of 1mg/ml catalyst to it and recorded UV-Vis spectra at regular time intervals as shown in figure 26.

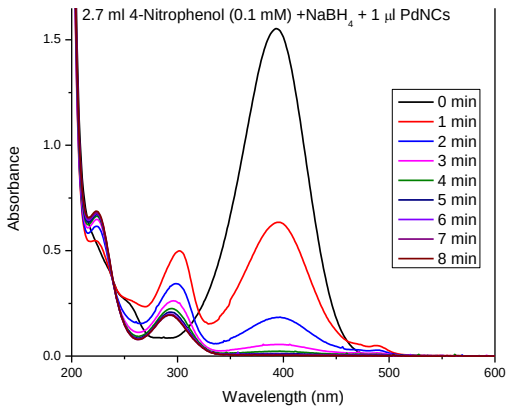

Fig 26. UV visible spectra showing reduction of 4-Nitrophenol + Sodium borohydride solution when catalyst was added to it.

For obtaining above spectra (Figure 26), we used the palladium nanostructures which were closest to cubic shape. That is, we used 22.5 mg $PdCl_2$, 3 drops of conc. HCl, 1 gm PVP, 12.5 mmol NaI, 15 ml H_2O and 25 ml autoclave containing reaction mixture was kept at 200^oC for 2+ 10 hours. Aqueous dispersion of catalyst was prepared from 1mg of the dried sample in an Eppendorf. 1ml of water was added to it and sonicated for a long time to ensure that it was homogeneously dispersed. As we can clearly notice from the spectra, as time progresses, the intensity of reactant peak drastically vanishes. After 4 min, the peak at 400 nm is no longer visible. At the same time, the new peak that emerges at 298 nm corresponds to 4-Aminophenol. Along with this, the vanishing yellow color of the reaction mixture also signifies the progression of the reaction.

Once we verified that the reaction is proceeding well in short interval of time, our next aim was to calculate the rate constant of our NCs and compare it with that of other nanostructures that we have synthesized and some literature reports.

Rate constant of reaction when different catalysts are used can be calculated in multiple steps. Firstly, we need to obtain Kinetics spectrum of reaction using UV Spectrophotometer as we can see from Figure 27.

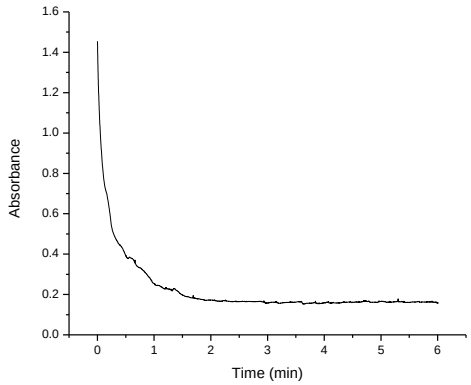

Fig 27. Kinetics spectrum of 4-Nitrophenol reduction using Palladium nanocubes

Next step is to plot ln (A_t/A_0) vs time (Figure 28). Slope of the steep part of the curve gives rate constant (k) of the reaction. Its unit would be inverse of the unit of time.

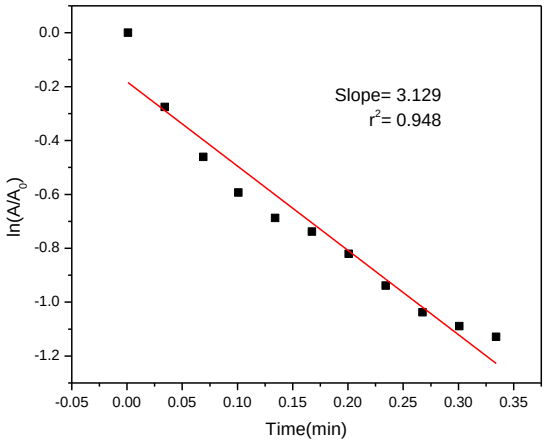

Fig 28. Plot of ln (A_t/A_0) vs time

Above graph gives a slope of -3.129. That is, rate constant is 3.129 min^{-1}. Similarly, Kinetics spectra were recorded for some other catalysts synthesized during the optimization process. In all of this set of nanostructures, we used 22.5 mg $PdCl_2$, 3 drops of conc. HCl, 1 gm PVP, 15 ml H_2O and 25 ml autoclave containing reaction mixture was kept at 200^oC. Only type and quantity of halide salt and time of nanostructure synthesis were varied. Reagents for 4-Nitrophenol reduction were kept same for all of these.

Catalyst specification	Rate constant (min^{-1})
NaI (x=2.5 mmol), 2h	0.254
NaI x, 2h	0.318
NaBr x/2 + SDS, 6 h	0.535
NaBr x, 2h	0.234
NaI 3x, 2 h	0.848
NaI x/3, 2h	0.429
NaI 5x, 2+6 h	**3.129**

NaI 5x, 8 h	1.379
NaI 7x, 8 h	0.486

Table 1. Rate constant for different palladium nanostructures generated during optimization process, for 4-Nitrophenol reduction

Catalyst	**[4-NP] (mM)**	**[cat.]**	**Time (sec.)**	**K (s^{-1})**
Pd–PRGO[37]	0.1	3 mg	15	0.24
Ni-Pt[38] (96:4)	0.0085	0.004 mg	60	0.116
Pd/RGO/Fe_3O_4[39]	1.2	5 mg	60	0.051
Porous Cu particle[40]	0.1	0.05 mg	390	0.0093
AuCu-MgO[41]	0.06	30 mg	1800	0.0003
Pd NWs[42]	0.09	0.3 mg	100	0.0194
Pd nanocube	**0.1**	**10 µg**	**20**	**0.052**

Table 2. Comparison of activity of different nanomaterials for 4-Nitrophenol reduction

From the tables 1 and 2, it is evident that Pd NCs show superior catalytic activity than other nanostructures synthesized along the way and other reported values.

3.3. Reduction of some other aromatic nitro compounds

3.3.1. 2-Nitrophenol

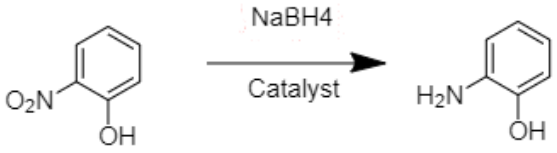

Fig 29. Schematic representation of 2-Nitrophenol reduction to 2- Aminophenol

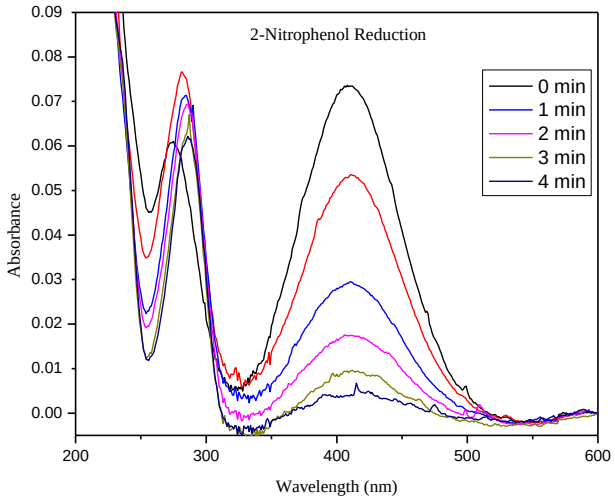

Fig 30. UV absorption spectra of 2-Nitrophenol reduction

3.3.2. 2,4-Dinitrophenol

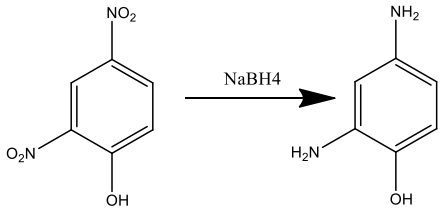

Fig 31. Schematic representation of 2,4-Dintrophenol reduction to Amidol

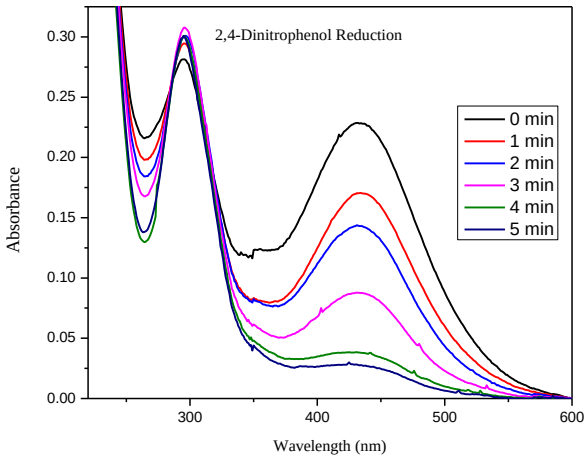

Fig 32. UV absorption spectra of 2,4-Dinitrophenol reduction

3.3.3. 3-Nitrophenol

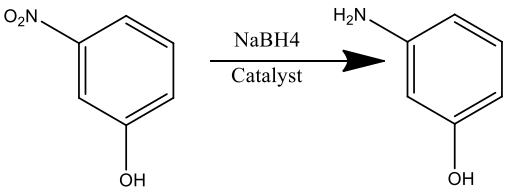

Fig 33. Schematic representation of 3-Nitrophenol reduction to 3-aminophenol

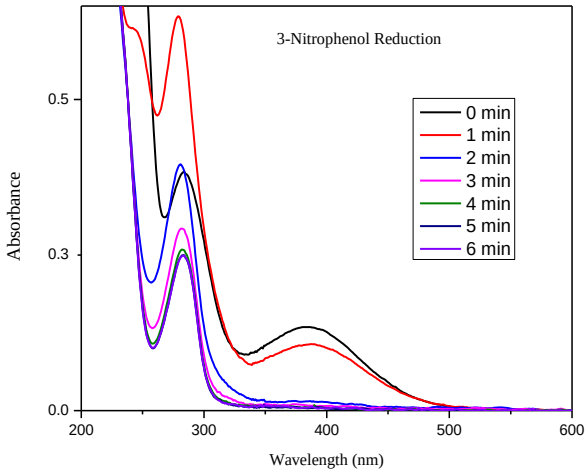

Fig 34. UV absorption spectra of 3-Nitrophenol reduction

3.3.4. 4-Nitroaniline

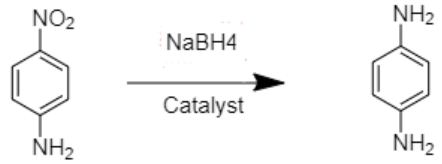

Fig 35. Schematic representation of 4-nitroaniline reduction to p-Phenylenediamine

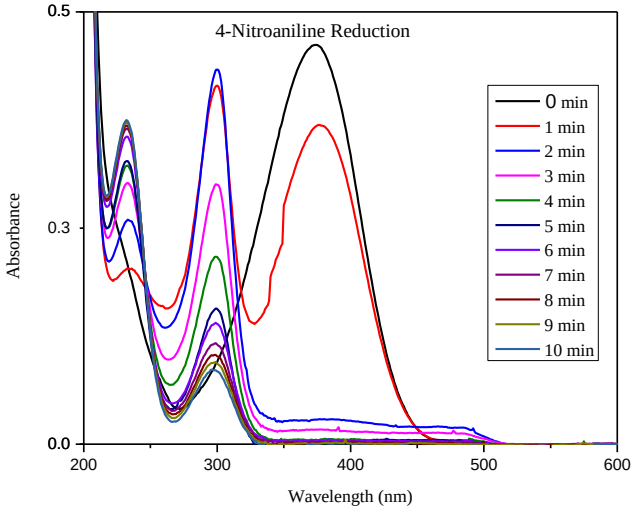

Fig 36. UV absorption spectra of 4-Nitroaniline reduction

3.3.5. 2-Hydroxy-5-nitrobenzaldehyde

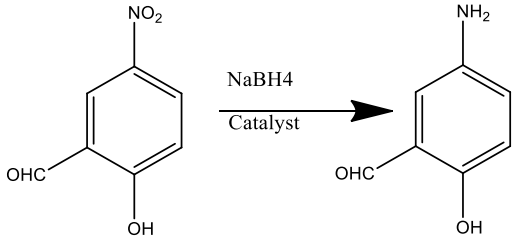

Fig 37. Schematic representation of reduction of 2-hydroxy-5-nitrobenzaldehyde, which is also known as 5-Nitrosalicylaldehyde to 5-Aminosalicylaldehyde

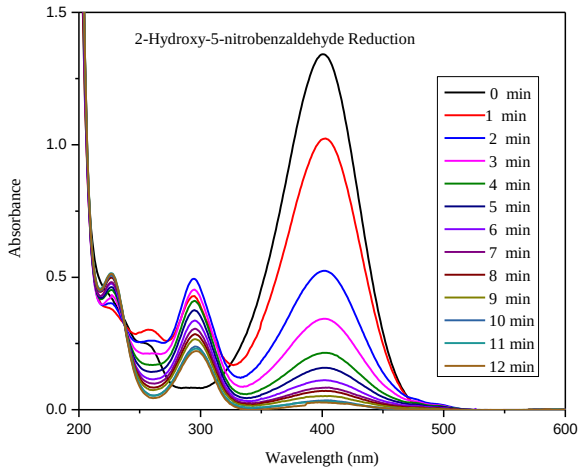

Fig 38. UV absorption spectra of 2-hydroxy-5-nitrobenzaldehyde reduction

3.3.6. Picric acid

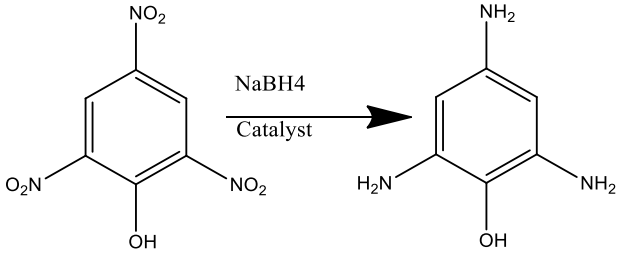

Fig 39. Schematic representation of reduction of picric acid to 2,4,6-triaminophenol

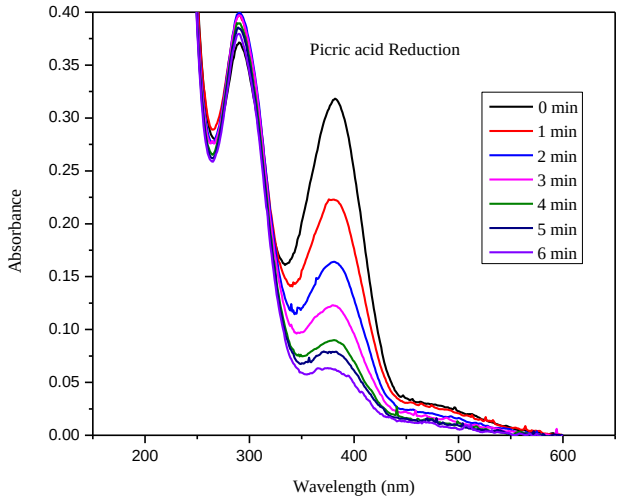

Fig 40. UV adsorption spectra of picric acid reduction

All of the above reactions were conducted at room temperature, with a substrate volume of 2.7 ml of 0.1 mM solution, Pd NCs amount of 1 µl from 1mg/ml aqueous dispersion and $NaBH_4$ solution of 0.3 ml taken from 0.6 M. In order to get kinetics spectra, we have taken 10 µl of catalyst dispersion, while other reaction conditions were kept same. Kinetic spectra were further utilized for estimating rate constant of the reaction catalyzed by obtained Pd NCs.

Compound	Rate constant(min^{-1})
2-Nitrophenol	0.490
2,4-Dinitrophenol	0.609
3-Nitrophenol	0.408
4-Nitroaniline	0.870
4-Nitrophenol	3.129
2-Hydroxy-5-nitrobenzaldehyde	0.573
Picric acid	1.112

Table 3. Rate constant for reduction of different aromatic nitro compounds using Palladium nanocubes

From the table 3, it is evident that Pd NCs can act as a good catalyst for the reduction of different aromatic compounds. Reduction of all aromatic nitro compounds will not take place at similar rates. This is due to the influence of some additional interactions. For instance, reduction of 2-Nitrophenol is more challenging than that of 4-Nitrophenol due to the presence of intra-molecular hydrogen bonding, which hinders adsorption of substrates onto the catalyst surface. When more substituents are present, steric hindrance also comes into picture. Para substitutes compounds can give better result than ortho- or meta- substituted compounds due to less steric hindrance.

Nevertheless, our catalyst reduces all the mentioned harmful aromatic nitro compounds into useful products at a remarkable rate.

3.4. Recyclability studies

Just verifying the catalytic activity is not good enough, we need to estimate the recyclability as well. Since palladium is a costly metal, if the synthesized catalyst has to be industrially manufactured, it has to maintain its efficiency after considerable amount of cycles. For this purpose, we took 4-Nitrophenol volume of 2.7 ml of 0.1 mM solution, Pd NCs amount of 10 µl from 1mg/ml aqueous dispersion and $NaBH_4$ solution of 0.3 ml taken from 0.6 M. After each cycle, 27µl of 10 mM of 4-Nitrophenol was added and the solution was mixed properly. From the drop in absorbance of reactant peak at 400 nm after each cycle, keeping a time fixed at 5.5 min (Time taken for 98.5% conversion in the first cycle), we can calculate the percentage of conversion of 4-Nitrophenol to 4-Aminophenol. For this, we will assume the initial absorbance just before the addition of catalyst as 100%. Once catalyst is added, the percentage of decrease in absorbance in accordance with time corresponds to the percentage of conversion. The result that we got is tabulated as table 4

Initial absorbance = 2.5	Absorbance at time= 5.5 min	Percentage of conversion
Cycle 1	0.0488	98.5 %
Cycle 2	0.0731	97.1 %
Cycle 3	0.0924	96.3 %
Cycle 4	0.204	91.8 %
Cycle 5	0.4253	82.98 %
Cycle 6	0.4676	81.3 %
Cycle 7	0.5862	76.55 %
Cycle 8	0.8663	65. 35 %
Cycle 9	1.15	54 %
Cycle 10	1.3591	45.6 %
Cycle 11	1.6408	34.36 %

Cycle 12	1.7361	30.56 %
Cycle 13	1.8607	25.57 %
Cycle 14	1.9299	22.8 %

Table 4. Percentage of conversion of 4- Nitrophenol reduction to 4-Aminophenol after repeated cycles

Above table can be consolidated into following graph (Figure 41).

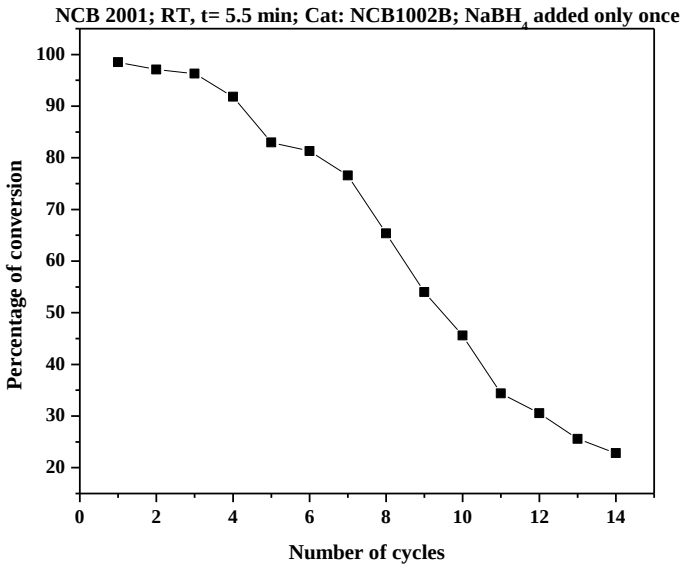

Fig 41. Recyclability of Palladium nanocubes for 4-Nitrophenol reduction

The catalytic activity does not decrease much up to three cycles and then it shows gradual decrease. By the end of 14th cycle, the percentage was decreased to 22.8 %, which was 98.5 % at the first cycle. Usually reaction dynamics will become more facile as we raise temperature. To check whether temperature can improve the recyclability of catalyst, we have performed the same set of reactions at an elevated temperature of 50^{o}C and got results as following (Figure 42):

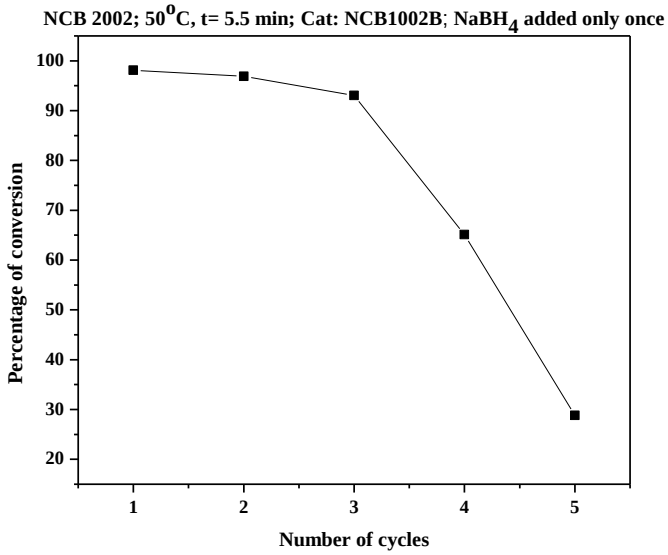

Fig 42. Recyclability of Palladium nanocubes for 4-Nitrophenol reduction at 50°C

Figure 42 shows that, contrary to our expectations, catalyst shows poor performance at elevated temperature. For first three cycles, similar trend as before can be observed, where percentage of conversion is pretty much high and does not vary much. But from then on, the scenario was drastically changed. While it shows 82.98 % conversion after 5 cycles at room temperature, the value was reduced to 28.8% for same number of cycles at 50°C. This might be due to many reasons. For instance,

1. While transferring to cuvette and beaker back and forth, there might be some catalyst loss.
2. $NaBH_4$ acts as hydride source for 4-Nitrophenol reduction. As we increase temperature, H_2 evolution will be more facile.

Any of these reasons or all of them collectively can be cumbersome to the progress of the reaction. To check whether our assumptions are true or not, we decided to redo the reactions at room temperature and high temperature by adding solid $NaBH_4$ after each cycle. Usually we use 300 µl of 0.6 M aqueous $NaBH_4$ solution. Since we were going to add solid $NaBH_4$ after each cycle, addition of this much excess may result in catalyst poisoning. So, we decided to add solid $NaBH_4$ corresponding to 0.3 ml of 0.3M of its

aqueous solution, that is, 3.45 mg. All the reactions were performed in cuvette to avoid any catalyst loss while transferring.

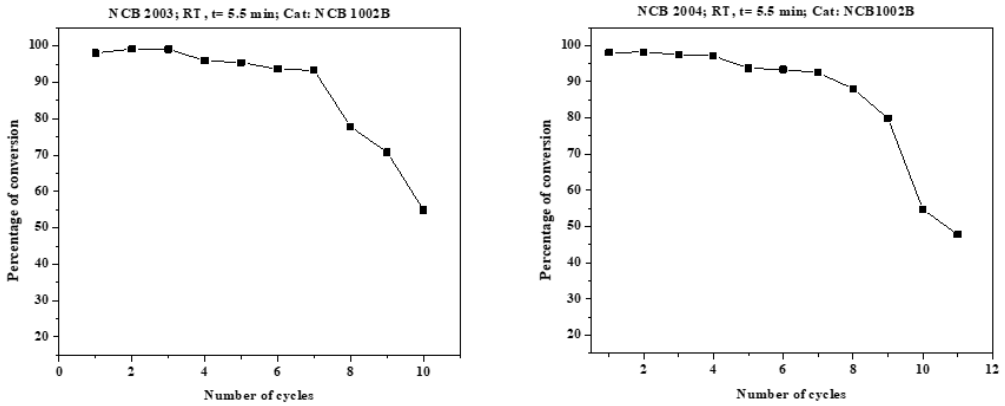

Fig 43. Recyclability of Palladium nanocubes for 4-Nitrophenol reduction at room temperature when $NaBH_4$ is added after each cycle

Addition of $NaBH_4$ only once turns out to be one of the reasons for the reduction in catalytic activity after repeated cycles. As we can see from the above graphs (Figure 43), high percentage of conversion can be observed up to 7 cycles. Sudden decline after 7^{th} cycle may be due to catalytic poisoning caused by the excess amount of borate complex formed which can occupy active sites of palladium nanostructures. It can also be because of large time interval between consecutive cycles of reaction. To check whether the second possibility can be ruled out or not, we have conducted the same set of experiments continuously at room temperature. Consecutive cycles were initiated by the addition of 4-Nitrophenol solution, once yellow color of reaction mixture from previous cycle was no longer visible.

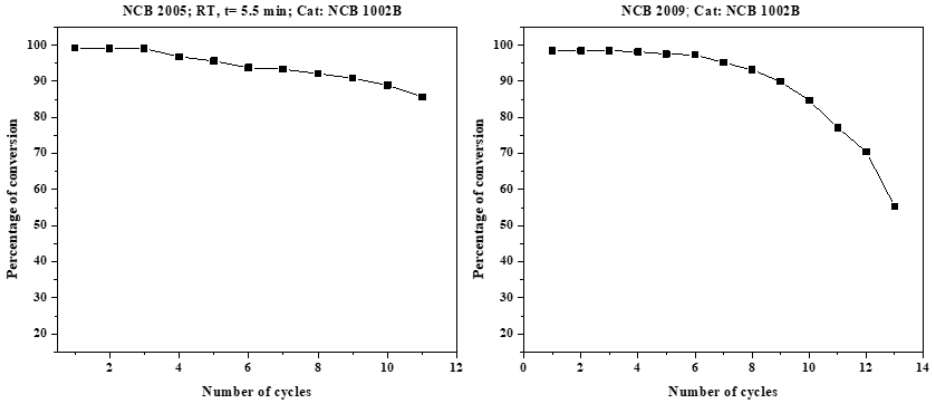

Fig 44. Recyclability of Palladium nanocubes for 4-Nitrophenol reduction at room temperature when $NaBH_4$ is added after each cycle without giving time gap between cycles

Above graphs (Figure 44) indicate that recyclability was indeed dependent on time gap between consecutive cycles. This might be because, longer we keep, more H_2 will evolve from the solution, which limits the amount of hydride ions required for the reaction. The exact reason has to be elucidated through further mechanistic studies. At high temperature, one more challenge is present i.e., evaporation is more apparent. This will bring down volume of the solvent (water), thereby increasing the concentration of substrate. In order to compensate the solvent loss, required amount of solvent was added to the reaction mixture after each cycle. Other reaction conditions were kept same as that of those at room temperature, along with the addition of Sodium borohydride after each cycle.

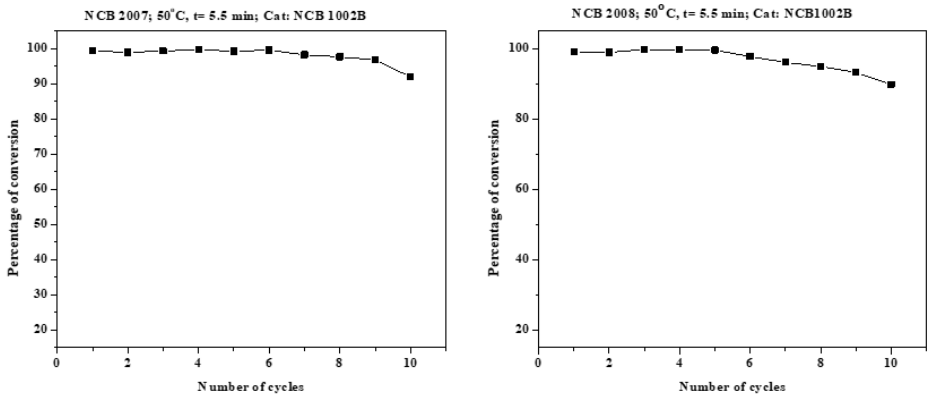

Fig 45. Recyclability of Palladium nanocubes for 4-Nitrophenol reduction at 50°C when $NaBH_4$ is added after each cycle

High percentage of conversion can be observed from repeated cycles at 50°C which ensures that the Pd NCs are indeed good catalyst for 4-Nitrophenol reduction.

3.5. Suzuki-Miyaura coupling reactions using as synthesized catalyst

As we have already discussed in the introduction, development and advancement of Suzuki-Miyaura coupling reactions have been center of attraction for organic chemists since very long time due to their various applications. So, if we can able to show that our Pd NCs can catalyze these reactions at better rate, it would be really helpful in different fields of Chemistry. With that aim in mind we have performed three sets of reactions with electron withdrawing, donating substrates and substrate without any of these two.

Reaction conditions: ArI (1mmol), $ArB(OH)_2$ (1.2 mmol), K_2CO_3 (2 mmol), $EtOH/H_2O$ (1:1, 4 ml) in the presence of Pd NCs (250 µl of aqueous dispersion corresponding to 0.3 mg Pd) at room temperature.

To optimize the reaction conditions of Suzuki- Miyaura coupling reaction, 4-iodobenzene and phenylboronic acid are commonly chosen as a model reaction. In most cases, oxidative addition is the rate-determining step of the catalytic cycle. I-Ph has low bond dissociation enthalpy when compared to that of other halides bonded with phenyl group. This makes coupling reactions more feasible. This is the reason why we chose Iodobenzene over Bromobenzene or Chlorobenzene. While choosing solvent, we have to be extra careful. If we take Water as a solvent, organic substrates cannot be completely dissolved in it. This will hamper the rate and yield of the reaction. Choosing organic solvent will also pose problem as inorganic base that we use will not dissolve properly. So, we decided to use EtOH- H_2O mixture at the ratio 1:1, that can be further optimized, if required. The usage of the co-solvent will ensure the good solubility of the inorganic base and the organic reactants. In terms of aqueous base to activate the boronate ester component, we have a long list of choice involving organic and inorganic bases such as, NaOH, $NaHCO_3$, K_2CO_3, K_3PO_4, KOH, NEt_3, and so on. Usually, organic base like NEt_3 are less reactive than inorganic bases such as K_2CO_3 and KOH. But high alkalinity of KOH makes it corrosive and very difficult to handle. Due to this problem, we decided to use K_2CO_3 as base for facilitating this reaction. Temperature plays an important role in bringing down kinetic barrier of the reaction. We decided to start at room temperature and see the effect. Surprisingly, at room temperature itself, our catalyst provided very high

yield in short time span. Usually for heterogeneous reactions, high temperature and phase transfer catalyst are necessary for reaction to take place. But in our case, without these two, we could attain high yield without even taking much time. This verifies the superior catalytic activity of Pd NCs over other required catalysts, most of which require an optimum temperature range of 70°C to 80°C to catalyze the reaction. Random amount of catalyst was used to verify whether reaction is going on or not. Further optimization of the amount of catalyst is still going on.

3.5.1. Substrate without electron donating or withdrawing group

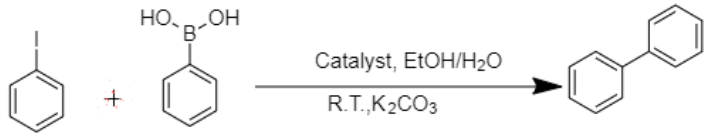

Fig 46. Reaction scheme for Suzuki-Miyaura coupling reaction using Iodobenzene and Phenyl boronic acid

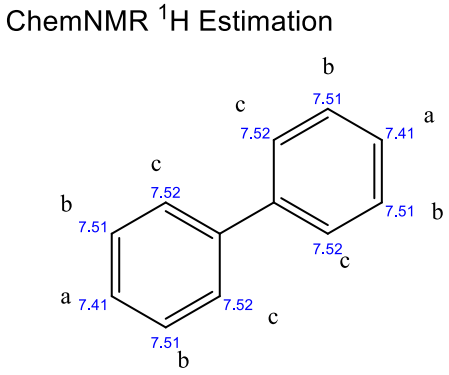

Fig 47. Estimated positions of peaks in ^{1}H NMR spectrum of 1,1'-biphenyl using ChemDraw software

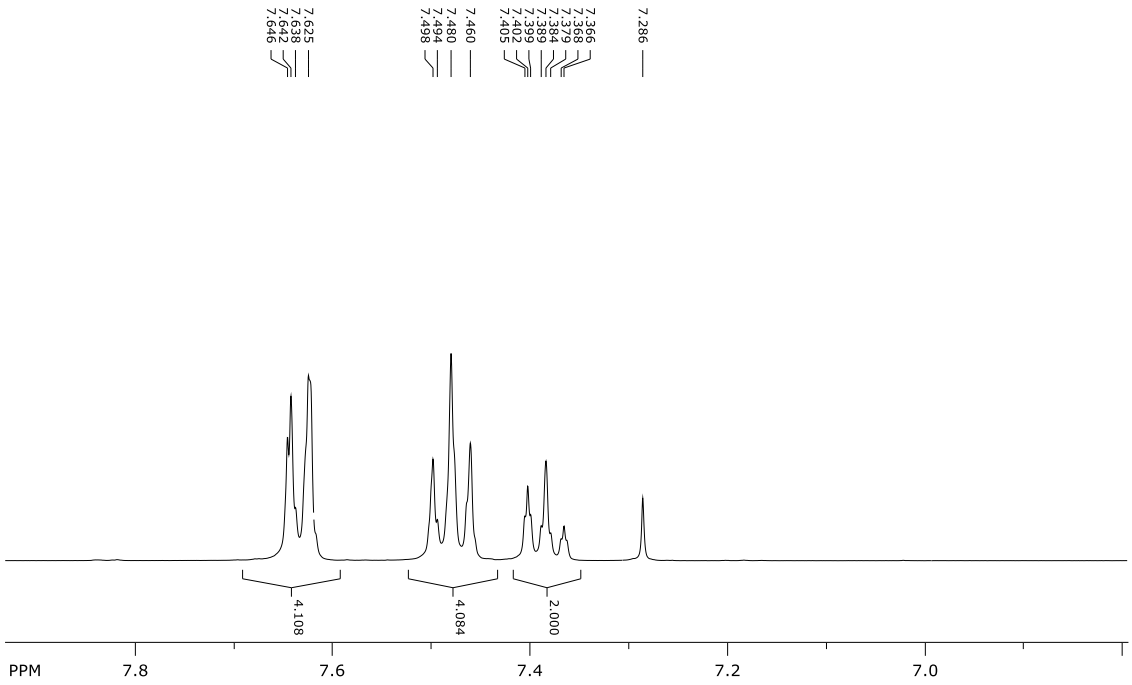

Fig 48. ^{1}H NMR spectrum of 1,1'-biphenyl

By using ChemDraw software, we can estimate the presence of three sets of peaks. ^{1}H NMR spectrum at room temperature shows four sets of peaks, one of which (singlet at 7.286 ppm) belongs to solvent $CDCl_3$. Total number of protons was obtained by integrating the peaks and it was found to be 10, which corresponds to the total number of protons of expected product. Triplet of triplet found around 4.366-4.4 ppm corresponds to that of proton (a) as shown in estimated figure shown before. Similarly, presence of peaks around 7.6 and 7.5 ppm corresponds to (b) and (c) respectively, which further verifies the structure.

Entry	Halide	Catalyst	Solvent	Time (h)	Yield (%)	TOF * (h^{-1})
1	Br	Pd $(PPh_3)_4$[43]	DME: H_2O (1.5:4.5)	-	88	34
2	Br	Pd (0) particles[44]	H_2O	2	7	-
3	Br	Pd nanorods in mesoporous channel of SBA-15[45]	EtOH/H_2O (1:1)	1.5	93.6	-

4	I	Pd immobilized mesoporous silica material[46]	MeOH	24	74	88
5	I	1,2,3- Triazolylidene Pd complex[47]	H_2O	12	94	-
6	I	Pd-$SnS_{reduced}$[48]	EtOH	24	97.4	-
7	**I**	**Pd nanocubes**	**EtOH/H_2O (1:1)**	**1.5**	**90**	**212.4**

*TOF= Turnover frequency

Table 5. Comparison of time taken, yield and TOF for Suzuki- Miyuara coupling using Palladium nanocubes with other reported catalysts when substrate without electron donating or withdrawing group is used.

3.5.2. Substrate with electron withdrawing group

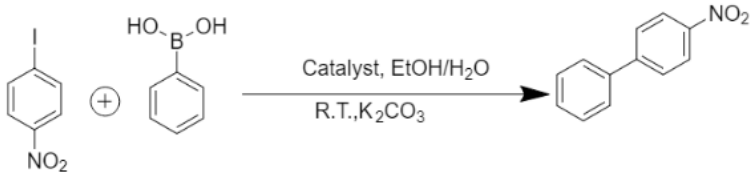

Fig 49. Reaction scheme for Suzuki-Miyaura coupling reaction using 1-Iodo-4-nitrobenzene and Phenyl boronic acid

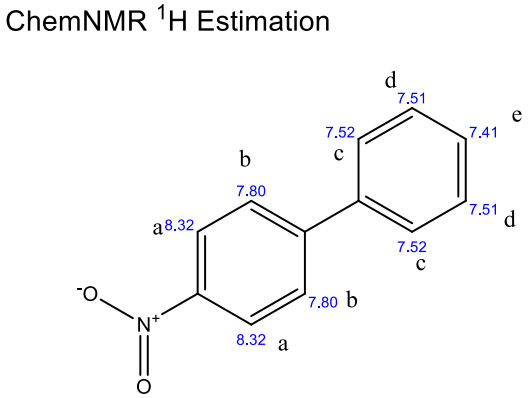

Fig 50. Estimated positions of peaks in 1H NMR spectrum of 4-nitro-1,1'-biphenyl using ChemDraw software

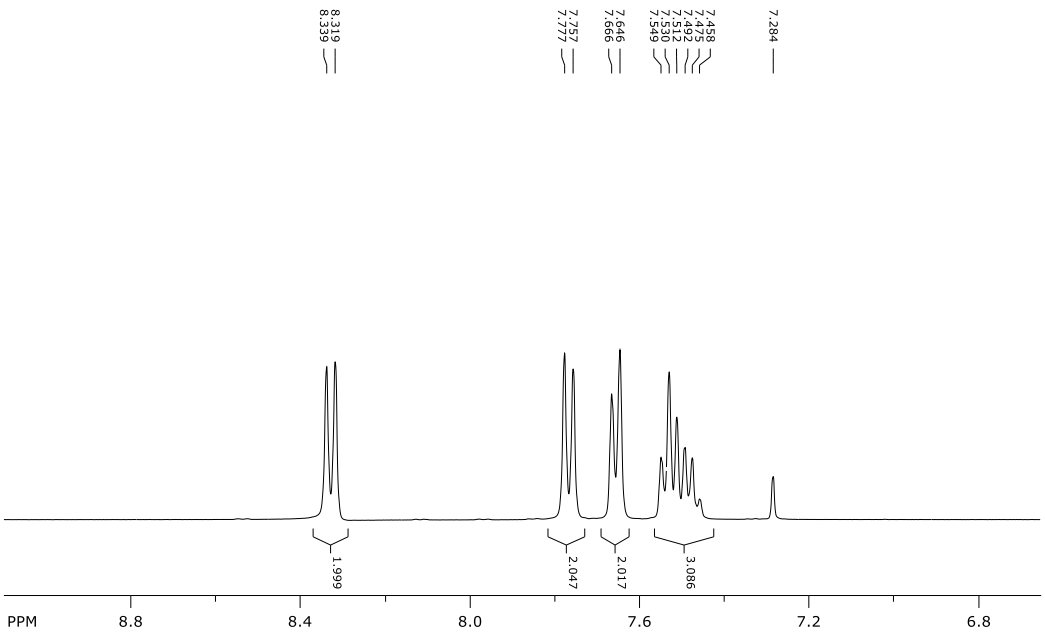

Fig 51. ^{1}H NMR spectrum of 4-nitro-1,1'-biphenyl

^{1}H NMR spectrum at room temperature shows five sets of peaks, one of which (singlet at 7.284 ppm) belongs to solvent $CDCl_3$. Total number of protons was obtained by integrating the peaks and it was found to be 9, which corresponds to the total number of protons of expected product. Doublet found around 8.3 ppm corresponds to that of proton (a) as shown in estimated figure shown before. Similarly, presence of doublets around 7.7 and 7.6 ppm corresponds to (b) and (c) respectively. The peaks of (c) and (d) are spread in 7.46-7.55 ppm range will merge together to form multiplet. The obtained NMR spectrum verifies the structure.

Entry	Halide	Catalyst	Solvent	Time (h)	Yield (%)	TOF (h^{-1})
1	Cl	Pd_1Ni_4/CNF**[49]	EtOH/H_2O (1:1)	5	6.32	-
2	Br	Pd (0) particles[50]	H_2O	2	6	-

3	Br	Pd nanorods in mesoporous channel of SBA-15[51]	EtOH/H_2O (1:1)	1.5	91.4	-
4	I	Pd immobilized mesoporous silica material[52]	MeOH	24	66	17
5	I	Pd Nanoparticles in ionic liquid[53]	H_2O	2	87	21.75
6	I	**Pd nanocubes**	**EtOH/H_2O (1:1)**	**16**	**90**	**19.92**

*TOF= Turnover Frequency

**CNF= Carbon Nano Fiber

Table 6. Comparison of time taken, yield and TOF for Suzuki- Miyuara coupling using Palladium nanocubes with other reported catalysts when substrate with electron withdrawing group is used.

3.5.3. Substrate with electron donating group

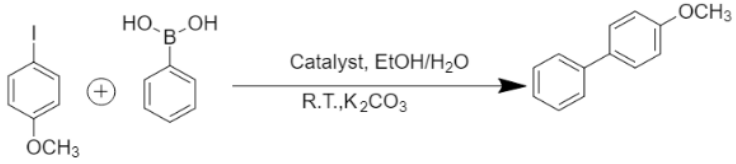

Fig 52. Reaction scheme for Suzuki-Miyaura coupling reaction using 4-Iodoanisole and Phenyl boronic acid

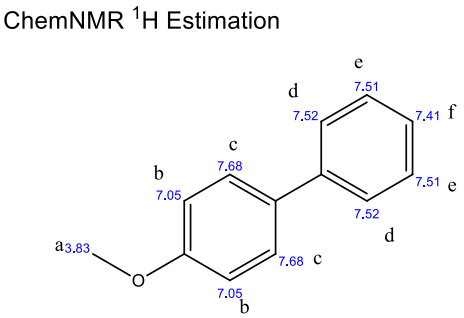

Fig 53. Estimated positions of peaks in 1H NMR spectrum of 4-methoxy-1,1'-biphenyl using ChemDraw software

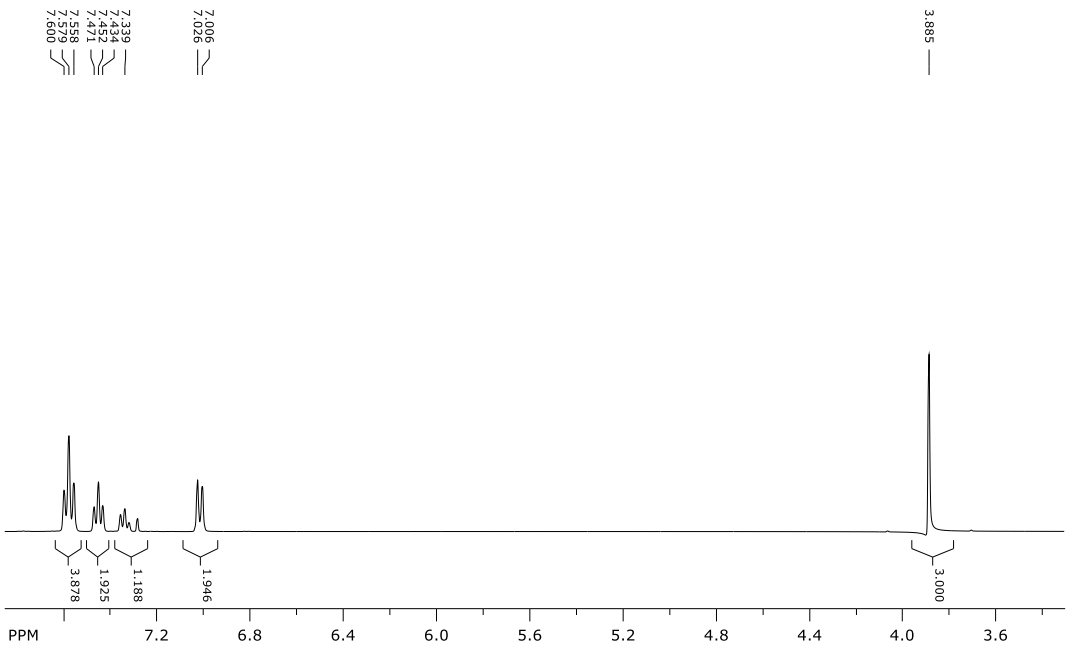

Fig 54. ^{1}H NMR spectrum of 4-methoxy-1,1'-biphenyl

^{1}H NMR spectrum at room temperature shows five sets of peaks. Total number of protons was obtained by integrating the peaks and it was found to be 12, which corresponds to the total number of protons of expected product. Singlet found around 3.88 ppm corresponds to that of proton (a) as shown in estimated figure shown before. Similarly, presence of triplets around 7.55-7.6, 7.47 and 7.05 ppm correspond to (c, d), (e) and (b) respectively. The multiplet at 7.339 ppm corresponds to (f) along with the trace amount of solvent $CDCl_3$. The obtained NMR spectrum verifies the structure.

Entry	Halide	Catalyst	Solvent	Time (h)	Yield (%)	TOF* (h^{-1})
1	Br	Pd nanorods in mesoporous channel of SBA-15[51]	EtOH/H_2O (1:1)	1.5	91.6	-

2	Br	Pd_1Ni_4/CNF**[54]	EtOH/H_2O (1:1)	3	98.77	263
3	I	Pd immobilized mesoporous silica material[52]	MeOH	24	75	88
4	I	Pd/CuO[55]	EtOH/H_2O (1:1)	1.5	31	-
5	I	Pd Nanoparticles in ionic liquid[56]	H_2O	1.5	88	29.33
6	I	**Pd nanocubes**	**EtOH/H_2O (1:1)**	**1.25**	**90**	**255**

*TOF= Turnover Frequency

**CNF= Carbon Nano Fiber

Table 7. Comparison of time taken, yield and TOF for Suzuki- Miyuara coupling using Palladium nanocubes with other reported catalysts when substrate with electron donating group is used.

In all of the above cases, when we used Pd NCs as catalyst, biphenyl products corresponding to aryl iodides containing both electron-withdrawing and electron-donating groups when coupled with phenylboronic acid, were obtained in excellent yields. Pd NCs that we have synthesized excels the previously reported catalysts in terms of shorter reaction times, higher stability and also better isolated yields. Further optimization of chemical parameters including solvent, kind of base, reaction temperature, amount of catalyst, catalyst loading on different templates like filter paper, sponge, silica, etc. and type of aryl halide substrate are still going on in our lab to determine the best possible combination. Filtration, purification and recycling of the catalyst are the main focus of the work that is currently going on.

4. Conclusion

Our aim was to use hydrothermal method for the efficient synthesis of Pd NCs. In order to understand the mechanism involved in the synthesis, we took UV-Vis spectra of reaction mixture at each step of the synthesis. From this study, we found that H_2PdCl_4 will be generated from $PdCl_2$ once conc. HCl is added. Addition of aqueous KI solution will replace chloride ions to generate H_2PdI_4. Under hydrothermal treatment at 200^oC for optimized amount of time, Palladium in +2 oxidation state will be reduced to Pd (0) and rearrange to form Pd NCs. Absence of any halide ions will generate palladium nanoparticles without any particular shape. So, we tried using different halide salts and noticed that KI is the best for the generation of NCs. Once we fixed the salt, we further tried different amounts of it to fix the optimum concentration required. Further optimization of time of hydrothermal treatment was also carried out. The as prepared nanostructures were further characterized by FESEM and TEM to verify their shape and dispersity.

Once Pd NCs were synthesized, our next aim was to check its catalytic activity. 4-Nitrophenol reduction to 4-Aminophenol was used as the model reaction for this purpose due to the ease of conducting reaction, calculating rate constant. The reaction is very important as well since 4- Nitrophenol is highly toxic and curbing its amount is necessary in current context. At the same time, the reduced product is highly beneficial in the synthesis of many drugs, dyes and so on. We verified the superior catalytic activity of our NCs over other synthesized nanostructures with the help of UV-Vis spectroscopy. Pd NCs showed a rate constant of 3.129 min^{-1}, which is far better than many catalysts that have been reported so far. Such a high activity may be due to the presence of large number of active sites on the edges of the cubes. We further verified the catalytic activity using other aromatic nitro compounds as well.

Since Palladium precursor is not so cheap, our catalyst can be industrialized only when if it can be recycled and reused many times without losing catalytic activity significantly. To check the recyclability, we conducted repeated cycles of 4-Nitrophenol reduction using

Pd NCs. When we tried to perform reaction at both room temperature and elevated temperature of 50^{o}C, after adding excess $NaBH_4$ only at the beginning of first cycle, we found drastic decrease in reduction of catalytic activity on repeating cycles due to the depletion of hydride ions from the solution due to hydrogen evolution. From this we concluded that $NaBH_4$ has to added after each cycle. Same set of reactions were conducted by adding it after each cycle showed that our catalyst was showing high efficiency even after many cycles.

Discovery of Suzuki-Miyaura coupling reaction is considered as one of the important milestones in the history of synthetic organic chemistry. Several modifications were introduced since its discovery. Still many limitations are still there. For example, homogeneous catalysts cannot be properly recycled and reused, while heterogeneous catalysts can catalyze the coupling only at elevated temperature and phase transfer catalyst is required. From our series of reactions, we discovered that Pd NCs can catalyze this reaction at room temperature in short time period providing high yield of coupled product without any side reactions. At the same time, phase transfer catalyst was not required due to the usage of cosolvents. The catalyst maintains very good activity when electron donating or withdrawing substituents were attached to the substrate as well.

5. Scope of the work

Through this project, we attempted to investigate the role of structure of metal nanoparticle in the enhancement of catalytic activity. Since noble metals are expensive, we need to develop suitable strategies where we can minimize the amount of metal as well as maximize its catalytic efficiency. Here comes the relevance of shape selective syntheses of nanostructures. As we have seen through this work, certain shapes can expose certain facets more, and thus we can tune the amount of exposed active sites and catalytic activity accordingly.

This thesis throws light on the superior catalytic activity of Pd NCs for 4-Nitrophenol reduction and Suzuki coupling over many other reported works. Minute quantity of catalyst can give very high yields of product due to the presence of {100} facets, which have low activation energy, thus favoring dissociative chemisorption of substrates.

Usage of Pd NCs does not end here. Through extensive experiments and studies, we can discover many catalytic reactions that can be catalyzed by it. For instance, Palladium metal nanoparticles are known for its excellent electrocatalytic activity[57]. We can extend the study to investigate the usage of Pd NCs for electrocatalytic water splitting[58], Carbon dioxide reduction[59] [60], Nitrogen fixation and so on. The potential applications of Pd NCs are infinitely vast.

6. Reference

(1) Xie, X.; Gao, G.; Pan, Z.; Wang, T.; Meng, X.; Cai, L. Large-Scale Synthesis of Palladium Concave Nanocubes with High-Index Facets for Sustainable Enhanced Catalytic Performance. *Sci. Rep.* **2015**, *5*, 8515.

(2) Kwawu, C. R.; Tia, R.; Adei, E.; Dzade, N. Y.; Catlow, C. R. A.; de Leeuw, N. H. CO2 Activation and Dissociation on the Low Miller Index Surfaces of Pure and Ni-Coated Iron Metal: A DFT Study. *Phys. Chem. Chem. Phys.* **2017**, *19* (29), 19478–19486. https://doi.org/10.1039/c7cp03466k.

(3) Johnston, R. L. Chapter 1 - Metal Nanoparticles and Nanoalloys. In *Metal Nanoparticles and Nanoalloys*; Johnston, R. L., Wilcoxon, J. P. B. T.-F. of N., Eds.; Elsevier, 2012; Vol. 3, pp 1–42. https://doi.org/https://doi.org/10.1016/B978-0-08-096357-0.00006-6.

(4) Kim, K.-S.; Demberelnyamba, D.; Lee, H. Size-Selective Synthesis of Gold and Platinum Nanoparticles Using Novel Thiol-Functionalized Ionic Liquids. *Langmuir* **2004**, *20* (3), 556–560. https://doi.org/10.1021/la0355848.

(5) Raza, A. M.; Kanwal, Z.; Rauf, A.; Sabri, N. A.; Riaz, S.; Naseem, S. Size- and Shape-Dependent Antibacterial Studies of Silver Nanoparticles Synthesized by Wet Chemical Routes. *Nanomaterials* . 2016. https://doi.org/10.3390/nano6040074.

(6) Dobrin, S. CO Oxidation on Pt Nanoclusters, Size and Coverage Effects: A Density Functional Theory Study. *Phys. Chem. Chem. Phys.* **2012**, *14* (35), 12122–12129. https://doi.org/10.1039/C2CP41286A.

(7) Collins, G.; Schmidt, M.; O'Dwyer, C.; Holmes, J. D.; McGlacken, G. P. The Origin of Shape Sensitivity in Palladium-Catalyzed Suzuki–Miyaura Cross Coupling Reactions. *Angew. Chemie Int. Ed.* **2014**, *53* (16), 4142–4145. https://doi.org/10.1002/anie.201400483.

(8) Ludwig, J. R.; Schindler, C. S. Catalyst: Sustainable Catalysis. *Chem* **2017**, *2* (3), 313–316. https://doi.org/https://doi.org/10.1016/j.chempr.2017.02.014.

(9) Li, J.; Zhao, T.; Chen, T.; Liu, Y.; Ong, C. N.; Xie, J. Engineering Noble Metal Nanomaterials for Environmental Applications. *Nanoscale* **2015**, *7* (17), 7502–7519.

https://doi.org/10.1039/C5NR00857C.

(10) Wang, L.; Tang, F.; Ozawa, K.; Chen, Z.-G.; Mukherj, A.; Zhu, Y.; Zou, J.; Cheng, H.-M.; Lu, G. Q. (Max). A General Single-Source Route for the Preparation of Hollow Nanoporous Metal Oxide Structures. *Angew. Chemie* **2009**, *121* (38), 7182–7185. https://doi.org/10.1002/ange.200900539.

(11) Jin, M.; Zhang, H.; Xie, Z.; Xia, Y. Palladium Concave Nanocubes with High-Index Facets and Their Enhanced Catalytic Properties. *Angew. Chemie Int. Ed.* **2011**, *50* (34), 7850–7854. https://doi.org/10.1002/anie.201103002.

(12) Zhang, J.; Zhang, L.; Xie, S.; Kuang, Q.; Han, X.; Xie, Z.; Zheng, L. Synthesis of Concave Palladium Nanocubes with High-Index Surfaces and High Electrocatalytic Activities. *Chem. – A Eur. J.* **2011**, *17* (36), 9915–9919. https://doi.org/10.1002/chem.201100868.

(13) Wang, C.; Wang, L.; Long, R.; Ma, L.; Wang, L.; Li, Z.; Xiong, Y. Anisotropic Growth of Palladium Twinned Nanostructures Controlled by Kinetics and Their Unusual Activities in Galvanic Replacement. *J. Mater. Chem.* **2012**, *22* (17), 8195–8198. https://doi.org/10.1039/C2JM30411B.

(14) Xia, X.; Choi, S.-I.; Herron, J. A.; Lu, N.; Scaranto, J.; Peng, H.-C.; Wang, J.; Mavrikakis, M.; Kim, M. J.; Xia, Y. Facile Synthesis of Palladium Right Bipyramids and Their Use as Seeds for Overgrowth and as Catalysts for Formic Acid Oxidation. *J. Am. Chem. Soc.* **2013**, *135* (42), 15706–15709. https://doi.org/10.1021/ja408018j.

(15) Huang, X.; Zhang, H.; Guo, C.; Zhou, Z.; Zheng, N. Simplifying the Creation of Hollow Metallic Nanostructures: One-Pot Synthesis of Hollow Palladium/Platinum Single-Crystalline Nanocubes. *Angew. Chemie Int. Ed.* **2009**, *48* (26), 4808–4812. https://doi.org/10.1002/anie.200900199.

(16) Niu, W.; Zhang, L.; Xu, G. Shape-Controlled Synthesis of Single-Crystalline Palladium Nanocrystals. *ACS Nano* **2010**, *4* (4), 1987–1996. https://doi.org/10.1021/nn100093y.

(17) Wu, J.; Zhao, J.; Qian, H.; Yue, L.; Guo, Y.; Fang, W. Deep Insights into the Growth Pattern of Palladium Nanocubes with Controllable Sizes. *RSC Adv.* **2016**, *6* (70), 66048–

66055. https://doi.org/10.1039/C6RA13163H.

(18) Xiong, Y.; Cai, H.; Wiley, B. J.; Wang, J.; Kim, M. J.; Xia, Y. Synthesis and Mechanistic Study of Palladium Nanobars and Nanorods. *J. Am. Chem. Soc.* **2007**, *129* (12), 3665–3675. https://doi.org/10.1021/ja0688023.

(19) Yang, T.-H.; Gilroy, K. D.; Xia, Y. Reduction Rate as a Quantitative Knob for Achieving Deterministic Synthesis of Colloidal Metal Nanocrystals. *Chem. Sci.* **2017**, *8* (10), 6730–6749. https://doi.org/10.1039/C7SC02833D.

(20) Sajanlal, P. R.; Sreeprasad, T. S.; Samal, A. K.; Pradeep, T. Anisotropic Nanomaterials: Structure, Growth, Assembly, and Functions. *Nano Rev.* **2011**, *2* (1), 5883. https://doi.org/10.3402/nano.v2i0.5883.

(21) Bhattarai, N.; Khanal, S.; Velazquez-Salazar, J. J.; Jose-Yacaman, M. Advanced Electron Microscopy in the Study of Multimetallic Nanoparticles BT - Advanced Transmission Electron Microscopy: Applications to Nanomaterials; Deepak, F. L., Mayoral, A., Arenal, R., Eds.; Springer International Publishing: Cham, 2015; pp 59–91. https://doi.org/10.1007/978-3-319-15177-9_3.

(22) Niu, W.; Li, Z.-Y.; Shi, L.; Liu, X.; Li, H.; Han, S.; Chen, J.; Xu, G. Seed-Mediated Growth of Nearly Monodisperse Palladium Nanocubes with Controllable Sizes. *Cryst. Growth Des.* **2008**, *8* (12), 4440–4444. https://doi.org/10.1021/cg8002433.

(23) Rabenau, A. The Role of Hydrothermal Synthesis in Preparative Chemistry. *Angew. Chemie Int. Ed. English* **1985**, *24* (12), 1026–1040. https://doi.org/10.1002/anie.198510261.

(24) Hamidouche, S.; Bouras, O.; Zermane, F.; Cheknane, B.; Houari, M.; Debord, J.; Harel, M.; Bollinger, J.-C.; Baudu, M. Simultaneous Sorption of 4-Nitrophenol and 2-Nitrophenol on a Hybrid Geocomposite Based on Surfactant-Modified Pillared-Clay and Activated Carbon. *Chem. Eng. J.* **2015**, *279*, 964–972. https://doi.org/10.1016/j.cej.2015.05.012.

(25) Aditya, T.; Pal, A.; Pal, T. Nitroarene Reduction: A Trusted Model Reaction to Test Nanoparticle Catalysts. *Chem. Commun.* **2015**, *51* (46), 9410–9431.

https://doi.org/10.1039/C5CC01131K.

(26) Xu, D.; Diao, P.; Jin, T.; Wu, Q.; Liu, X.; Guo, X.; Gong, H.; Li, F.; Xiang, M.; Ronghai, Y. Iridium Oxide Nanoparticles and Iridium/Iridium Oxide Nanocomposites: Photochemical Fabrication and Application in Catalytic Reduction of 4-Nitrophenol. *ACS Appl. Mater. Interfaces* **2015**, *7* (30), 16738–16749. https://doi.org/10.1021/acsami.5b04504.

(27) Lv, J.-J.; Wang, A.-J.; Ma, X.; Xiang, R.-Y.; Chen, J.-R.; Feng, J.-J. One-Pot Synthesis of Porous Pt–Au Nanodendrites Supported on Reduced Graphene Oxide Nanosheets toward Catalytic Reduction of 4-Nitrophenol. *J. Mater. Chem. A* **2015**, *3* (1), 290–296. https://doi.org/10.1039/C4TA05034G.

(28) Ahmed Zelekew, O.; Kuo, D.-H. A Two-Oxide Nanodiode System Made of Double-Layered p-Type Ag2O@n-Type TiO2 for Rapid Reduction of 4-Nitrophenol. *Phys. Chem. Chem. Phys.* **2016**, *18* (6), 4405–4414. https://doi.org/10.1039/C5CP07320K.

(29) Chawla, M.; Kumar, R.; Siril, P. F. High Catalytic Activities of Palladium Nanowires Synthesized Using Liquid Crystal Templating Approach. *J. Mol. Catal. A Chem.* **2016**, *423*, 126–134. https://doi.org/https://doi.org/10.1016/j.molcata.2016.06.014.

(30) Matos, K.; Soderquist, J. A. Alkylboranes in the Suzuki−Miyaura Coupling: Stereochemical and Mechanistic Studies. *J. Org. Chem.* **1998**, *63* (3), 461–470. https://doi.org/10.1021/jo971681s.

(31) Das, T.; Uyama, H.; Nandi, M. Pd-Bound Functionalized Mesoporous Silica as Active Catalyst for Suzuki Coupling Reaction: Effect of OAc^-, PPh3 and Cl^- Ligands on Catalytic Activity. *J. Solid State Chem.* **2018**, *260*, 132–141. https://doi.org/10.1016/J.JSSC.2018.01.027.

(32) Amatore, C.; Jutand, A.; Le Duc, G. Kinetic Data for the Transmetalation/Reductive Elimination in Palladium-Catalyzed Suzuki–Miyaura Reactions: Unexpected Triple Role of Hydroxide Ions Used as Base. *Chem. – A Eur. J.* **2011**, *17* (8), 2492–2503. https://doi.org/10.1002/chem.201001911.

(33) Smith, G. B.; Dezeny, G. C.; Hughes, D. L.; King, A. O.; Verhoeven, T. R. Mechanistic

Studies of the Suzuki Cross-Coupling Reaction. *J. Org. Chem.* **1994**, *59* (26), 8151–8156. https://doi.org/10.1021/jo00105a036.

(34) Yuan, Q.; Zhuang, J.; Wang, X. Single-Phase Aqueous Approach toward Pd Sub-10 Nm Nanocubes and Pd–Pt Heterostructured Ultrathin Nanowires. *Chem. Commun.* **2009**, No. 43, 6613–6615. https://doi.org/10.1039/B913974E.

(35) Shanthi, K.; Vimala, K.; Gopi, D.; Kannan, S. Fabrication of a PH Responsive DOX Conjugated PEGylated Palladium Nanoparticle Mediated Drug Delivery System: An in Vitro and in Vivo Evaluation. *RSC Adv.* **2015**, *5* (56), 44998–45014. https://doi.org/10.1039/C5RA05803A.

(36) Chen, W.; Yang, X.; Long, G.; Wan, X.; Chen, Y.; Zhang, Q. A Perylene Diimide (PDI)-Based Small Molecule with Tetrahedral Configuration as a Non-Fullerene Acceptor for Organic Solar Cells. *J. Mater. Chem. C* **2015**, *3* (18), 4698–4705. https://doi.org/10.1039/C5TC00865D.

(37) Yang, M.-Q.; Pan, X.; Zhang, N.; Xu, Y.-J. A Facile One-Step Way to Anchor Noble Metal (Au, Ag, Pd) Nanoparticles on a Reduced Graphene Oxide Mat with Catalytic Activity for Selective Reduction of Nitroaromatic Compounds. *CrystEngComm* **2013**, *15* (34), 6819–6828. https://doi.org/10.1039/C3CE40694F.

(38) Ghosh, S. K.; Mandal, M.; Kundu, S.; Nath, S.; Pal, T. Bimetallic Pt–Ni Nanoparticles Can Catalyze Reduction of Aromatic Nitro Compounds by Sodium Borohydride in Aqueous Solution. *Appl. Catal. A Gen.* **2004**, *268* (1), 61–66. https://doi.org/https://doi.org/10.1016/j.apcata.2004.03.017.

(39) Atarod, M.; Nasrollahzadeh, M.; Mohammad Sajadi, S. Green Synthesis of Pd/RGO/Fe3O4 Nanocomposite Using Withania Coagulans Leaf Extract and Its Application as Magnetically Separable and Reusable Catalyst for the Reduction of 4-Nitrophenol. *J. Colloid Interface Sci.* **2016**, *465*, 249–258. https://doi.org/https://doi.org/10.1016/j.jcis.2015.11.060.

(40) Wang, J.; Wu, Z.; Li, T.; Ye, J.; Shen, L.; She, Z.; Liu, F. Catalytic PVDF Membrane for Continuous Reduction and Separation of P-Nitrophenol and Methylene Blue in Emulsified

Oil Solution. *Chem. Eng. J.* **2018**, *334*, 579–586. https://doi.org/https://doi.org/10.1016/j.cej.2017.10.055.

(41) Liu, X.; Li, Y.; Xing, Z.; Zhao, X.; Liu, N.; Chen, F. Monolithic Carbon Foam-Supported Au Nanoparticles with Excellent Catalytic Performance in a Fixed-Bed System. *New J. Chem.* **2017**, *41* (24), 15027–15032. https://doi.org/10.1039/C7NJ03018E.

(42) Sahoo, L.; Rana, M.; Mondal, S.; Mittal, N.; Nandi, P.; Gloskovskii, A.; Manju, U.; Topwal, D.; Gautam, U. K. Self-Immobilized Pd Nanowires as an Excellent Platform for a Continuous Flow Reactor: Efficiency, Stability and Regeneration. *Nanoscale* **2018**, *10* (45), 21396–21405. https://doi.org/10.1039/C8NR06844E.

(43) Chen, Z.; Vorobyeva, E.; Mitchell, S.; Fako, E.; Ortuño, M. A.; López, N.; Collins, S. M.; Midgley, P. A.; Richard, S.; Vilé, G.; et al. A Heterogeneous Single-Atom Palladium Catalyst Surpassing Homogeneous Systems for Suzuki Coupling. *Nat. Nanotechnol.* **2018**, *13* (8), 702–707. https://doi.org/10.1038/s41565-018-0167-2.

(44) Verma, A.; Tomar, K.; Bharadwaj, P. K. Nanosized Bispyrazole-Based Cryptand-Stabilized Palladium(0) Nanoparticles: A Reusable Heterogeneous Catalyst for the Suzuki–Miyaura Coupling Reaction in Water. *Inorg. Chem.* **2019**, *58* (2), 1003–1006. https://doi.org/10.1021/acs.inorgchem.8b03015.

(45) Li, J.; Bai, X.; Lv, H. In-Situ Ultrasonic Synthesis of Palladium Nanorods into Mesoporous Channel of SBA-15 and Its Enhanced Catalytic Activity for Suzuki Coupling Reaction. *Microporous Mesoporous Mater.* **2019**, *275*, 69–75. https://doi.org/https://doi.org/10.1016/j.micromeso.2018.08.013.

(46) Das, T.; Uyama, H.; Nandi, M. Pronounced Effect of Pore Dimension of Silica Support on Pd-Catalyzed Suzuki Coupling Reaction under Ambient Conditions. *New J. Chem.* **2018**, *42* (8), 6416–6426. https://doi.org/10.1039/C8NJ00254A.

(47) Sasidharan, D.; Aji, C. V; Mathew, P. 1,2,3-Triazolylidene Palladium Complex with Triazole Ligand: Synthesis, Characterization and Application in Suzuki–Miyaura Coupling Reaction in Water. *Polyhedron* **2019**, *157*, 335–340. https://doi.org/https://doi.org/10.1016/j.poly.2018.10.022.

(48) Shan, X.; Sui, N.; Liu, W.; Liu, M.; Liu, J. In Situ Generation of Supported Palladium Nanoparticles from a Pd/Sn/S Chalcogel and Applications in 4-Nitrophenol Reduction and Suzuki Coupling. *J. Mater. Chem. A* **2019**, *7* (9), 4446–4450. https://doi.org/10.1039/C8TA11772A.

(49) Bao, G.; Bai, J.; Li, C. Synergistic Effect of the Pd–Ni Bimetal/Carbon Nanofiber Composite Catalyst in Suzuki Coupling Reaction. *Org. Chem. Front.* **2019**, *6* (3), 352–361. https://doi.org/10.1039/C8QO01100A.

(50) Verma, A.; Tomar, K.; Bharadwaj, P. K. Nanosized Bispyrazole-Based Cryptand-Stabilized Palladium(0) Nanoparticles: A Reusable Heterogeneous Catalyst for the Suzuki–Miyaura Coupling Reaction in Water. *Inorg. Chem.* **2019**, *58* (2), 1003–1006. https://doi.org/10.1021/acs.inorgchem.8b03015.

(51) Li, J.; Bai, X.; Lv, H. In-Situ Ultrasonic Synthesis of Palladium Nanorods into Mesoporous Channel of SBA-15 and Its Enhanced Catalytic Activity for Suzuki Coupling Reaction. *Microporous Mesoporous Mater.* **2019**, *275*, 69–75. https://doi.org/https://doi.org/10.1016/j.micromeso.2018.08.013.

(52) Das, T.; Uyama, H.; Nandi, M. Pronounced Effect of Pore Dimension of Silica Support on Pd-Catalyzed Suzuki Coupling Reaction under Ambient Conditions. *New J. Chem.* **2018**, *42* (8), 6416–6426. https://doi.org/10.1039/C8NJ00254A.

(53) Gaikwad, D. S.; Undale, K. A.; Patil, D. B.; Pore, D. M. Multi-Functionalized Ionic Liquid with in Situ-Generated Palladium Nanoparticles for Suzuki, Heck Coupling Reaction: A Comparison with Deep Eutectic Solvents. *J. Iran. Chem. Soc.* **2019**, *16* (2), 253–261. https://doi.org/10.1007/s13738-018-1503-z.

(54) Bao, G.; Bai, J.; Li, C. Synergistic Effect of the Pd–Ni Bimetal/Carbon Nanofiber Composite Catalyst in Suzuki Coupling Reaction. *Org. Chem. Front.* **2019**, *6* (3), 352–361. https://doi.org/10.1039/C8QO01100A.

(55) Fu, W.; Cao, Y.; Feng, Q.; Smith, W. R.; Dong, P.; Ye, M.; Shen, J. Pd–Co Nanoalloys Nested on CuO Nanosheets for Efficient Electrocatalytic N2 Reduction and Room-Temperature Suzuki–Miyaura Coupling Reaction. *Nanoscale* **2019**, *11* (3), 1379–1385.

https://doi.org/10.1039/C8NR08724E.

(56) Gaikwad, D. S.; Undale, K. A.; Patil, D. B.; Pore, D. M. Multi-Functionalized Ionic Liquid with in Situ-Generated Palladium Nanoparticles for Suzuki, Heck Coupling Reaction: A Comparison with Deep Eutectic Solvents. *J. Iran. Chem. Soc.* **2019**, *16* (2), 253–261. https://doi.org/10.1007/s13738-018-1503-z.

(57) Sarkar, S.; Peter, S. C. An Overview on Pd-Based Electrocatalysts for the Hydrogen Evolution Reaction. *Inorg. Chem. Front.* **2018**, *5* (9), 2060–2080. https://doi.org/10.1039/C8QI00042E.

(58) Li, J.; Li, F.; Guo, S.-X.; Zhang, J.; Ma, J. PdCu@Pd Nanocube with Pt-like Activity for Hydrogen Evolution Reaction. *ACS Appl. Mater. Interfaces* **2017**, *9* (9), 8151–8160. https://doi.org/10.1021/acsami.7b01241.

(59) Lüsi, M.; Erikson, H.; Sarapuu, A.; Tammeveski, K.; Solla-Gullon, J.; Feliu, J. M. *Oxygen Reduction Reaction on Carbon-Supported Palladium Nanocubes in Alkaline Media*; 2016; Vol. 64. https://doi.org/10.1016/j.elecom.2015.12.016.

(60) Erikson, H.; Sarapuu, A.; Kongi, N.; Tammeveski, K.; Solla-Gullon, J.; Feliu, J. M. *Electrochemical Reduction of Oxygen on Palladium Nanocubes in Acid and Alkaline Solutions*; 2012; Vol. 59. https://doi.org/10.1016/j.electacta.2011.10.074.